Cathode Beam Behavior in a High Speed Oscillograph

Thesis by

Arthur E. Harrison

In Partial Fulfillment of the Requirements

for

The Degree of Doctor of Philosophy

California Institute of Technology

Pasadena, California

1940

TABLE OF CONTENTS

ACKNOWLEDGMENT

The assistance offered by Dr. R. W. Sorensen and all members of the Electrical Engineering faculty of the California Institute of Technology is very gratefully acknowledged. Dr. Fred Lindvall should be thanked in particular for constant encouragement and frequent advice. A suggestion by Dr. R. B. Brode at the University of California led to the explanation of transient gas focusing. Dr. Howard Griest authorized the use of certain illustrations from his thesis to describe the equipment used, and Bernard Oliver and V. C. Rideout often assisted in obtaining data.

SUMMARY

High speed cathode-ray oscillographs utilizing high vacuum tubes and external photography are now available, but certain electrical research problems require writing speeds in excess of those possible with such equipment. A moderately low voltage, cold cathode type, high-speed oscillograph for internal photography is part of the Institute High Voltage Laboratory. Its capabilities beyond the range possible with the present high vacuum tubes have been investigated. The factors affecting its operation were studied, and the results of this study have suggested improvements in the equipment, as well as furnishing data of considerable practical value and theoretical interest.

Distortion affecting the magnitude and direction of deflection of the beam has been eliminated and distortions affecting the size and shape of the beam spot have been reduced. Transient gas focusing in the tube has not been eliminated, but the factors causing transient gas focusing have been studied, and a tentative explanation of the phenomenon is suggested. The operation of the oscillograph as an electron microscope is described. The principles of electron optics are used to explain the observed results when an axial magnetic field is used to increase the ratio of the beam current to the total discharge current. The effects of gas and vapor pressure, cathode surface conditions and cathode age on the operation of the oscillograph are described. The writing speed of the oscillograph was extended somewhat and was measured as 2×10^9 cm. per second. Published papers made possible by the improved operation of the oscillograph are included as an Appendix.

INTRODUCTION

Dependable high speed oscillograph equipment is an essential part of any electrical testing laboratory designed for high voltage measurements. Several high-speed oscillographs of the cold cathode type were constructed and operated in the Institute High Voltage Laboratory prior to the availability of commercial high-vacuum oscillograph tubes for high speed recording with an external camera. These cold cathode tubes have been described in doctor's theses by Griest[1], Hawley[2] and Pleasants[3]. Although high vacuum tubes with sufficient writing speed for lightning surge studies are now available, there is still a range of operation which is satisfied best by a cold cathode type oscillograph with internal film recording. The tube designed by Dr. Howard Griest was chosen for further development in 1936 because it was relatively simple to operate and required considerably less accelerating potential than other tubes used previously.

One of the principal uses of a high speed oscillograph is the recording of transients following the application of artificial lightning surges to electrical equipment. A surge generator which can be tripped mechanically is used in the Institute High Voltage Laboratory for impulse testing. Such a system requires an electrical connection between the surge generator and the oscillograph for coordinating the two sets of equipment. The surge tripping mechanism, oscillograph trip connection and delay cable connecting the voltage divider across the test apparatus and the oscillograph deflection plates must be designed so the entire transient phenomenon may be recorded. Also, the oscillograph should not be disturbed by the electromagnetic field created by the surge generator. These requirements are difficult to attain completely,

but a satisfactory compromise was effected so that routine testing was possible.

Since impulse research as well as commercial testing was in progress almost continuously, it was necessary to carry out a development program without interfering with routine testing. At the same time, cathode beam behavior was studied in order to improve the oscillogram records. As a result, the cathode beam studies were often intimately related to the development of operating technique, so that no attempt has been made to separate the two factors, although the results may vary, from electron phenomena which are merely informative, to changes which concern purely mechanical improvements in the equipment. No radical changes in the design of the oscillograph were considered. The work was limited to an investigation of the factors affecting the optimum operation of the existing equipment.

EQUIPMENT

A continuous cathode beam is furnished by a metal discharge tube using a removable aluminum cathode and an anode with a 0.016 inch diameter window. Air is admitted by a needle valve leak to allow a cold discharge. The needle valve lead screw is drilled so the leaking gas or air can be controlled or passed through a drying tube if necessary, and the lead screw is lubricated with stopcock grease to prevent an inlet of air at that point. The details of the cathode assembly are given in Figure 2. A blocking chamber of Rogowski type is used to prevent fogging of the film while no record is being made. Additional details of the design of the oscillograph are given in the thesis by Dr. R. H. Griest[1].

Focusing of the beam is accomplished with two coils mounted in iron cases with a small air gap to give a concentrated field coaxial with the cathode beam. One coil is located above the sweep and deflection plates, approximately midway between the anode window and the screen, to form an image of the anode window at the screen and give the sharpest possible trace. The other coil has fewer turns of larger wire; it is located just above the anode, and is used as a fore-concentration coil to increase the number of electrons in the cathode beam. Current for both coils is obtained from a six-volt storage battery controlled by potentiometers.

Deflection normal to the sweep direction is caused by a pair of deflection plates approximately 40 cm. above the fluorescent screen. A selector switch mounted near the deflection plates connects these plates to different taps on the terminating impedance of the delay cable for impulse testing. An electron coupled radio-frequency oscillator furnishes a timing wave. Deflection sensitivity is measured with a d-c

voltage supply controlled by a set of tapped resistances and a 1000 ohm rheostat in series with the primary of the power transformer of the rectifier. A reversing switch for the high voltage supply was built into the tap switch on the control panel but was not connected into the circuit. A set of coils connected through a reversing switch to a potentiometer across the six-volt storage battery furnishes a magnetic bias to adjust the position of the cathode beam in the deflection direction.

Six different sweep speeds from less than one microsecond to several hundred microseconds duration can be selected by changing a tap switch. The sweep impulse is capacitively coupled to the sweep plates so that electrostatic bias can be used to control the position of the beam on the screen. A "heating circuit" consisting of several condensers and some resistance is often used to improve the spark at the trip gap. Such a circuit was discarded after a trial because no improvement was apparent when fast sweeps were used, and the circuit actually caused periodic reblocking with the slower sweeps.

Several 400 ohm resistors are required for damping oscillations in the L C circuits formed by the different plates and their leads. 400 ohm resistors are not quite high enough for critical damping, but they reduce the oscillations adequately. Very high frequency oscillations are apparent in the deflection plate circuit with the fastest sweeps, but they are small in amplitude and not objectionable, although they are relatively undamped. Other circuit values for the blocking and sweep circuits are given in Figure 3. Figure 4 gives the connections for all circuits on the main control panel.

No change was made in the camera and screen mechanism originally constructed by Dr. Griest. A description of this mechanism will not be repeated here, but a photograph of the camera is included as Figure 5.

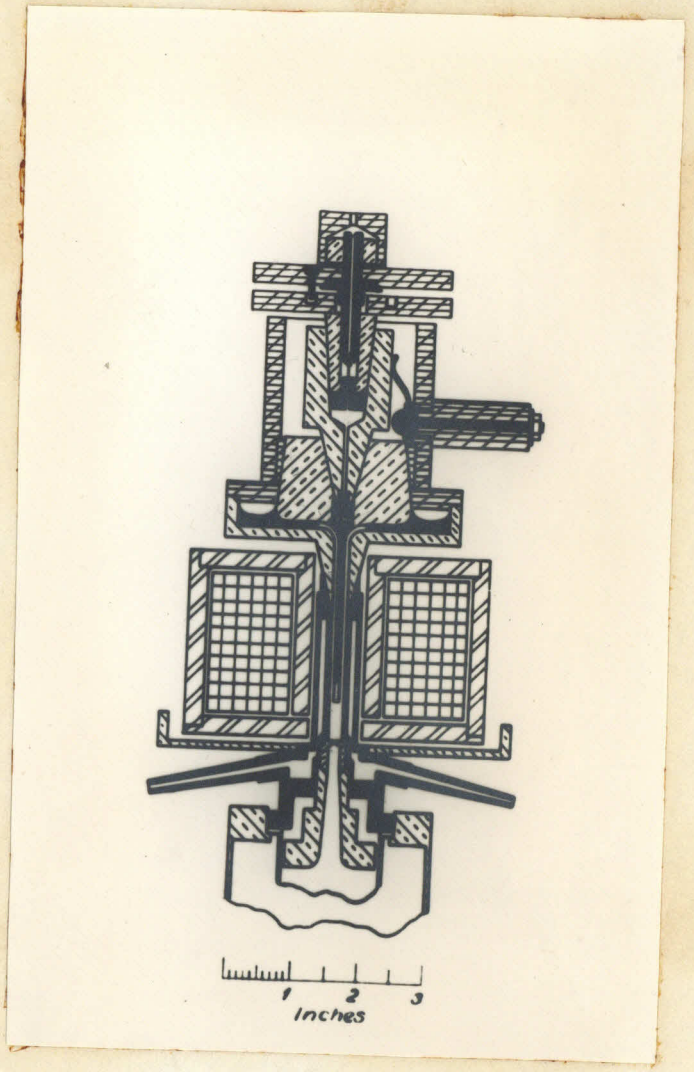

FIGURE 2

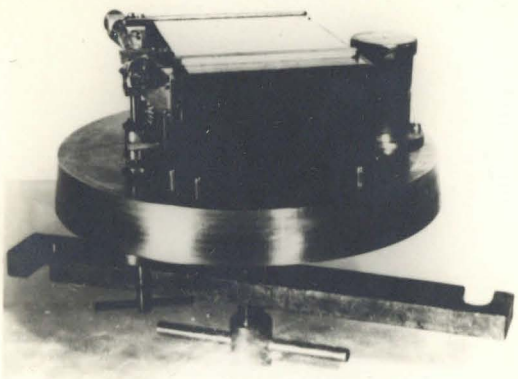

FIGURE 5

Table I

Terminal Numbers	Circuits
1 - 2 *	Earth's Field Compensation
3 - 4 *	Focus
5 - 6 *	Fore-concentration
7 - 8	Magnetic Bias
9 -10 *	Battery
11	Electrostatic Bias Filament
12	Electrostatic Bias Plate
13	Sweep Filament
14	Sweep Plate
15	A. C. Ground
16	Fore Pump
17	Vapor Pumps
18	Kenetron Filament
19	Kenetron Plate
20	A. C. Input
21	Glow Tube
22	A. C. Master Switch
23	Sensitivity Bias Plate
24	Not in use

* 2 - 4 - 6 - 10 D. C. Positive and common lead.

The oscillograph is constructed of brass and requires a coil surrounding the entire tube to nullify the effect of the earth's magnetic field. If not compensated, the magnetic field of the earth causes a deflection of approximately one inch and may deflect the discharge sufficiently to reduce appreciably the number of electrons passing through the limiting aperture below the anode window.

Three stages of mercury diffusion pumps and a Hyvac forepump are used continuously during operation. With the needle valve leak adjusted for normal discharge current, this pumping system will reach a pressure of 2×10^{-4} mm. of mercury. A shut-off valve between the oscillograph system and the pumps is provided. In addition, a glow tube operated by a 7500 volt neon sign transformer, a McLeod gauge, and an extra adjustable leak are connected to the vacuum lead in order to provide means of controlling and checking the vacuum in the system under any desired operating conditions. The glow tube gives an occasional flickering discharge at a pressure of 23 mm. of mercury; continuous discharge begins at a pressure of 20 mm. of mercury and the tube becomes dark again at approximately 2×10^{-2} mm. A recess in the top of the lowest pressure stage of the diffusion pumps serves as an adequate, although troublesome, liquid air trap requiring frequent refilling.

Several changes were made in the mechanical layout of the equipment to improve the ease of operation. The equipment was originally set up for preliminary testing on the south balcony in the Institute High Voltage Laboratory. Controls were of somewhat temporary construction. Experience in this first location indicated that static shielding of the oscillograph, or a location more remote from the surge generator, or perhaps both, would be desirable. Accordingly, a new location in the alcove under the main entrance to the building was selected because it would be more remote, and

if complete shielding were found necessary, the building itself would act as an effective shield so that minimum additional construction would be required.

At the same time, revision of the mounting and control apparatus was completed. Observing hoods with dark slides were added above the windows originally provided. The 10000 volt power supply was rebuilt more compactly with the filament transformer for the kenetron at ground potential and the high voltage transformer insulated for inverse peak voltage. A 5 milliampere meter, protected by a series resistor and a neon lamp, was placed in series with the 20 milliampere meter in order to give a more sensitive indication of discharge current. Wire wound limiting resistors in the lead to the discharge tube replaced the water column used previously. An a. c. operated solenoid was installed to discharge the high voltage filter condenser when the power was shut off. A self starting synchronous clock was installed to measure the cathode age, or length of time that a cathode had been in operation. Also, the high-voltage lead to the discharge tube was placed in a copper tubing conduit in order to shield the lead.

The coil for the fore-concentration field was rewound with larger wire so that a single six volt storage battery would be sufficient as a power source. A new compensating coil for the earth's magnetic field was wound, and the deflection bias coils were rewound to improve the uniformity of the magnetic field. The resistances of the various coils are tabulated below:

Earth Coil	30.0
Deflection Bias Coils	7.3
Focusing Coil	9.4
Fore Concentration Coil	5.0

All of the oscillograph equipment except the two storage batteries and the 10000 volt power supply is mounted in a single operating bench. Below the oscillograph are the d-c power supplies for the blocking system, sweep circuit bias, and deflection calibration voltage. A removable control panel is connected to a terminal block (Table I, following Figure 5) by a cord and combination of plugs so the controls may be examined without interfering with the operation of the oscillograph, or removed for changes or repairs and easily replaced. The vacuum pumps are beneath the data table. An electron coupled oscillator with a selector switch for a choice of 100 kc, 333 kc, 1000 kc, 3333 kc, or 10000 kc is beside the oscillograph, with its power supply directly below. Figure 1 shows the general arrangement of the operating bench.

PHOTOGRAPHY

Roll film with a relatively slow emulsion, sensitive only in the blue-violet region of the visible spectrum, proved to be most successful with this oscillograph. Such film (Eastman NC roll film) is quite sensitive to direct electron exposure; while at the same time it is relatively inexpensive, it can be handled easily because total darkness is not required during development; it is not fogged if the camera is opened when the operator's face against the viewing hood is the only shielding from the room lights.

Film ordinarily contains considerable moisture which must be removed before satisfactory operation of the oscillograph is possible. Phosphorous pentoxide will dehydrate the outer layers of paper surrounding the film, but continued pumping with a vacuum system is the only adequate method of preparing film for use. A separate vacuum system for this purpose would be desirable. Since none was readily available, a number of

films were placed in the oscillograph at one time and were pumped continuously for 24 hours or more until the films were dry. The mercury pumps were not used until the glow tube showed that the water vapor pressure had been reduced adequately. Dried films were stored in the oscillograph until they were required.

Two contrast emulsions were tested in the oscillograph. The results were similar in both cases; the slower sweeps gave an intense black trace but the faster sweeps were barely discernible. Photostat paper gave somewhat better results than process film, perhaps because this film had a thin gelatine coating to protect the emulsion. Photostat paper might have some advantages if a large number of oscillograms are to be made on one film. A roll film allows only 10 separate exposures, or 30 surge oscillograms per roll if the film is advanced only one-half turn between exposures. It is usually desirable to develop the film and examine the results after this number of exposures has been made, and the advantage of a greater number of oscillograms per roll becomes questionable. The fact that less moisture would be introduced by a roll of photostat paper would certainly be advantageous. The photostat paper might be removable in daylight if some scheme similar to that used with 35 mm. film were adopted. This suggestion might be worth further investigation.

The effect of emulsion thickness may have influenced these results. Emulsions on roll films vary between thicknesses of 7.5×10^{-4} cm. and 40×10^{-4} cm. The thickness of the photostat emulsion is less than these values but the actual thickness was not determined. The thickness of the emulsion and the protective coating on the process film is 1.4×10^{-4} cm. Wood[9] states that the penetration of electrons is proportional to the fourth power of the velocity. The maximum penetration is given by:

$$s = \frac{E_a^2}{4.04\ d \times 10^{11}} \qquad (224p) \quad Dow^4$$

E_a = accelerating voltage

d = density of medium penetrated

10000 volt electrons would therefore penetrate to a depth of 2.5×10^{-4} cm. or less than the total thickness of the emulsion on a roll film.

DEFLECTION DISTORTION

Distortion affecting the response of the beam to deflecting fields is of major importance, as a true picture of the electrical transient being recorded is desirable. Corrections might be applied to a distorted oscillogram, but this technique is definitely inferior to obtaining an oscillogram which represents, within the tolerance limits of the experiment, a linear relation between the measured deflection and the voltage transient. A linear sweep is not always necessary, however, and an exponential sweep voltage is used frequently.

Two methods of bias may be used to locate the beam on the screen. The beam may be deflected to any desired position with a magnetic field, or a fixed voltage may be applied to either pair of deflection plates. Condensers must be used to couple the deflection plates to the transient voltage if the latter method of electrostatic bias is used.

Originally, the sweep plates were connected directly to the sweep condensers, and a magnetic field was applied to return the beam to the screen. Two sets of coils furnished fields to deflect the beam in the deflection direction and along the sweep axis. These coils were 4 inches in diameter and were placed about 4 inches apart surrounding the region of the sweep plates. The magnetic field given by two coils spaced a distance equal to their diameter is illustrated by Figure 8. The lines of equal magnetic vector potential were found by graphical interpolation from

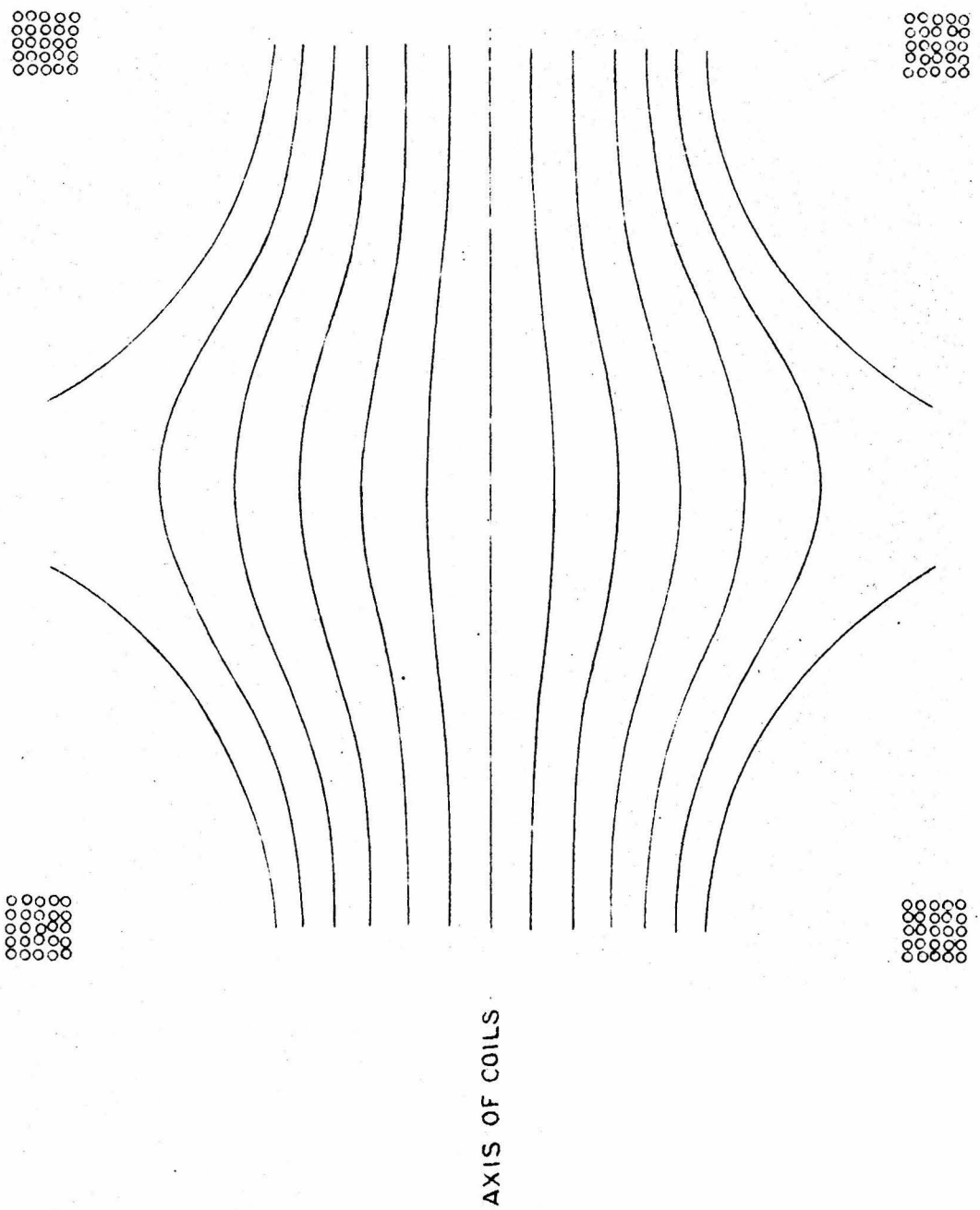

FIGURE 8

LINES OF EQUAL VECTOR POTENTIAL FOR TWO COILS SPACED TWICE THEIR RADIUS

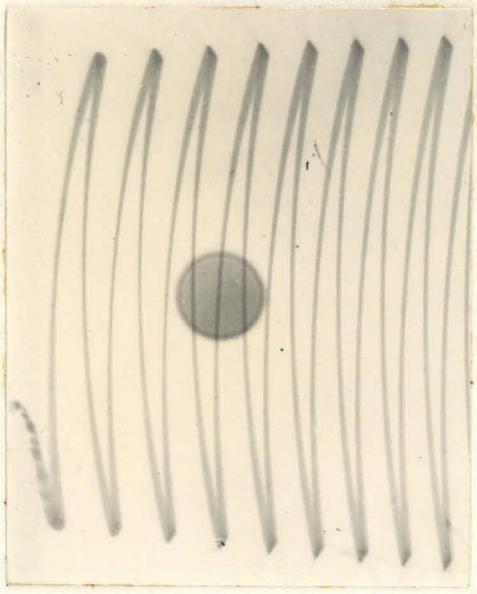

Figure 6
1 megacycle timing wave
Magnetic Bias

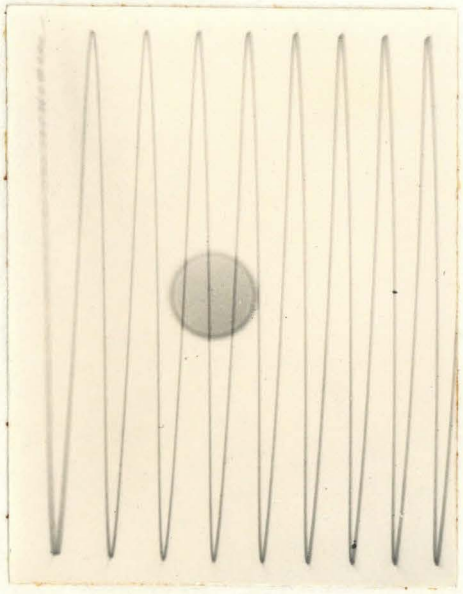

Figure 7
1 megacycle timing wave
Electrostatic Bias

computations of

$$A_{\phi} = \frac{4\mu}{k} I \left(\frac{a}{\rho}\right)^{\frac{1}{2}} \left[\left(1-\tfrac{1}{2}k^2\right)K-E\right] \qquad 7.04(4) \text{ Smythe}^5$$

where K and E are the complete elliptic integrals for the modulus k.

$k^2 = 4a\rho \left[(a-\rho)^2 + z^2\right]^{-1}$

a = radius of the loop

ρ = radial coordinate

z = distance from plane of loop

As a result of this non-uniform field, a sine wave deflection voltage is recorded as a warped, double valued function whose amplitude varies with position along the sweep axis. (Figure 6). The correct amplitude of the sine wave is given by Figure 7.

Any attempt to obtain an exact analysis of such distortion would be impractical, since the path of the beam at any point depends on the integrated effect of a magnetic and an electrostatic field, and neither field is uniform, or even exactly known. Most of the deflection caused by the electric field occurs near the top of the sweep plates; the plates are not parallel but diverge to prevent the beam from approaching the plates during the extremes of the sweep, since the beam is swept far beyond the left of the screen in order to allow reblocking before the sweep returns. The magnetic deflection along the sweep axis occurs more uniformly. Since the magnetic field increases on either side of the plane midway between two coils separated by a distance equal to twice their radius, the effect of the magnetic bias is greater as the beam is moved to either side of the zero axis by the deflection plates. This fact explains the crescent shape of the distortion. The amplitude is reduced because the magnetic deflection occurs in that part of the field to the left of the axis of the coils, where the field has a radial component in the

proper direction to account for the reduction in amplitude.

Comparison of Figures 6 and 7 shows that there is a slight net effect of the radial component of the magnetic field when the beam has swept to the right side of the axis of the coils, i.e., the radial components on opposite sides of the axis do not exactly compensate because the beam striking the center of the oscillogram leaves the magnetic and electric fields at the left of the central axis at such an angle that a continued straight path will intersect the center of the oscillogram. Note also that there is an elliptical distortion of the beam spot when the beam departs from the zero deflection axis. Such elliptical distortion of the beam always occurs in a non uniform field. In Figure 7 there is some slight crescent distortion at large amplitudes in the opposite direction to that previously discussed. This phenomenon is due to a non uniform electric field caused by the shape of the sweep plates and the fact that the sweep plates were not placed symmetrically in the oscillograph. The extreme deflections exaggerate the effect.

Deflection distortion increases at a greater than linear rate as the electrostatic and magnetic fields are increased simultaneously with small resultant motion of the beam to the left of the screen. It would be quite possible to reduce the effect satisfactorily by capacitively coupling the sweep plates to the sweep condensers, and shunting the sweep plates with a high resistance so the beam would normally begin its sweep at the center of the screen. A more uniform magnetic field from a Helmholtz arrangement of coils spaced equal to their radius could then be used to bias the starting point of the sweep to the left. However, with capacitive coupling it is possible to use an electrostatic bias which is easily controlled in magnitude with a potentiometer in the primary at the power supply transformer, and the beam may be biased com-

pletely to the left and the action of reblocking observed without the introduction of appreciable distortion.

In order to provide a convenient means of changing the position of the zero deflection axis, the coils for this purpose were rewound in a form vaguely resembling the intersection of a circular cylinder and an elliptical cylinder with a major axis twice the diameter of the circle and the minor axis of the ellipse. This form of coil gave a somewhat more uniform magnetic field but some distortion remained, although it is not important when deflections are small.

BEAM DISTORTION

Several types of distortion affect the size or shape of the focused spot. Although this beam distortion is not quite as important as deflection distortion, certain types of beam distortion proved very difficult to minimize. Fortunately, however, operating conditions can usually be chosen so that good oscillograms can be obtained over the entire range of operating requirements.

One unavoidable form of distortion caused by a non uniform field has been called elliptical distortion. Consider the effect of an electrostatic field, as illustrated in Figure 9, on a circular cathode beam of greater than infinitesimal diameter. If deflection is toward the ungrounded electrode, the electrons nearest that electrode are acted upon by a stronger field than that acting upon the electrons in the opposite side of the beam. The result is an elongation of the circular beam along the axis perpendicular to the electrodes. Reduction of the minor axis of the elliptical beam will be caused by the curvature of the electric field. Similarly, if the ungrounded electrode is negative, the circular beam will become elliptical with its major axis parallel

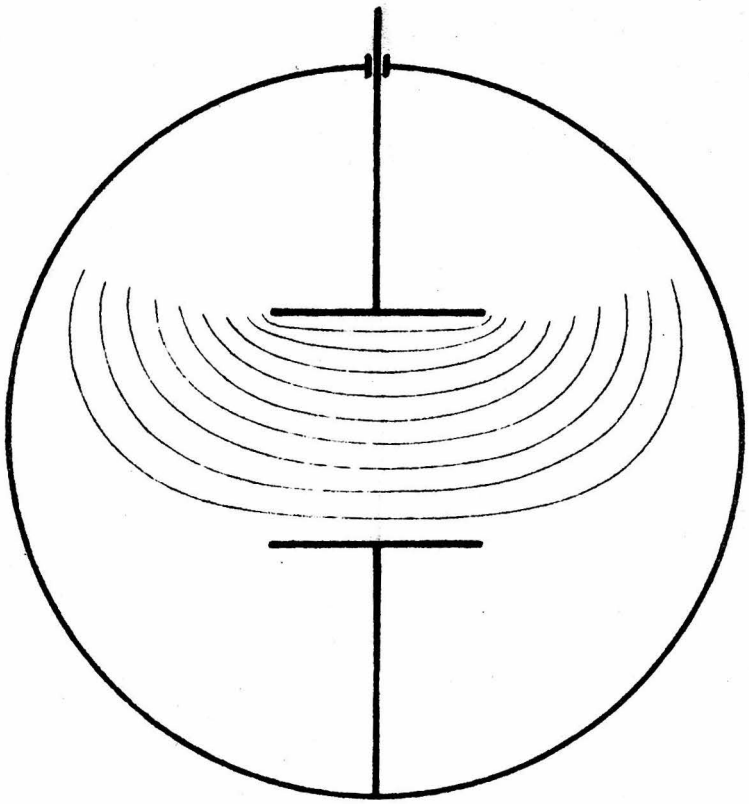

FIGURE 9

EQUIPOTENTIAL DIAGRAM
NARROW PLATES ONE PLATE GROUNDED

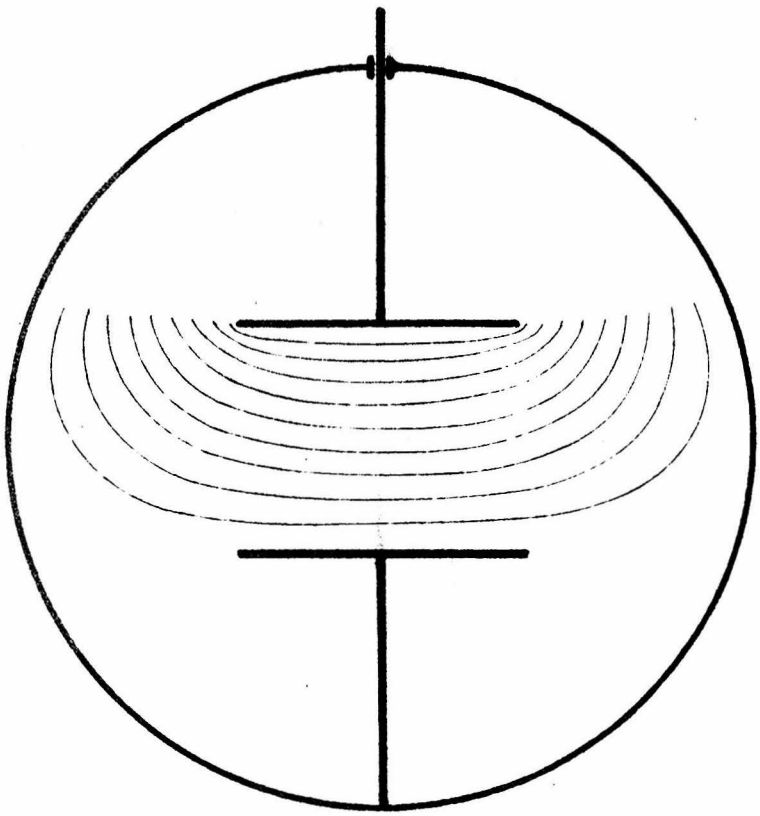

FIGURE 10

EQUIPOTENTIAL DIAGRAM
WIDER PLATES ONE PLATE GROUNDED

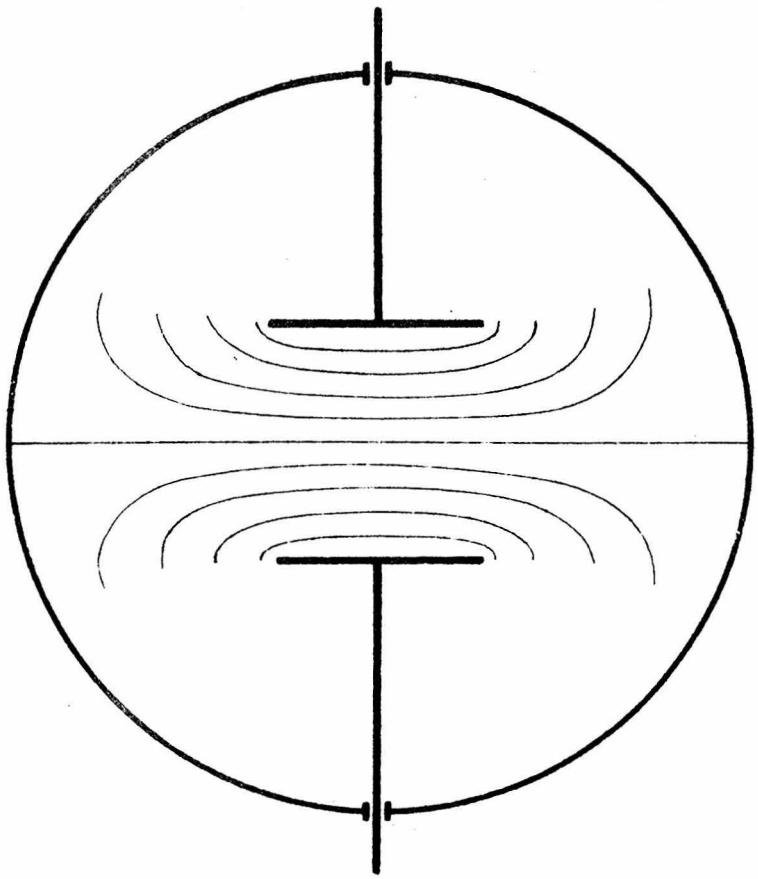

FIGURE 11

EQUIPOTENTIAL DIAGRAM
NARROW PLATES PLATES UNGROUNDED

to the electrodes. Focusing the beam would reduce the effect slightly, since the beam would have converged somewhat before entering the deflection field, but two focused lines appear for different values of focusing field current and a point focus cannot be obtained. The end effects introduced by the top and bottom of the plates increase this distortion considerably.

Certain applications of the oscillograph, particularly studies with a surge generator, require that one of the deflection plates be grounded. A non uniform deflection field is then unavoidable. While it is impossible to select any value of focusing field current which will give a narrow trace throughout the entire oscillogram, this distortion can be minimized by a proper design of the deflection plates. Deflection amplitude is proportional to the product of the field strength and the time that the field acts upon an electron if the amplitude is small. Increasing the length of the deflection plates will therefore reduce the field strength necessary for a given deflection amplitude and decrease the elliptical distortion by reducing the importance of the end effects introduced by the top and bottom of the plates. The uniformity of the field itself can be improved by closer spacing of the plates and/or widening the plates. Compare Figures 9 and 10. All of these factors were considered in the design of new deflection plates for the oscillograph.

Increasing the length of the deflection plates and reducing the spacing increase the capacity of the deflection system, which may not be important, and increase the deflection sensitivity of the oscillograph in addition to reducing the elliptical distortion when one plate is grounded. More than 1000 volts was required for a deflection of one inch prior to changing the deflection plates. Deflection sensitivity was more

than doubled by the change and it became practical to measure deflections corresponding to only 100 volts. This increased sensitivity was quite useful in tests of the blocking system and a paper, "Ionization Time of Thyratrons", contains some results of this investigation. A preprint of this paper is included as Appendix A.

Another paper, "Surge Voltage Breakdown Characteristics for Electrical Gaps in Oil", by Professor R. W. Sorensen, is included as Appendix B. Thousands of surge oscillograms were obtained for this investigation. These two papers are examples of two widely different types of routine tests that are possible with the oscillograph. Figure 12 shows a surge oscillogram and a superimposed timing wave. Note the greater sharpness of the timing wave trace which was made with the two plates symmetrical with respect to ground. A better illustration of the effect of symmetrical and unsymmetrical deflection voltages can be made by a comparison of the surge trace in Figure 12 and the much greater deflections in Figure 7.

An annoying form of beam distortion affecting the focus of the beam during sweep, first observed in early tests of the oscillograph, is illustrated in Figure 13. If the beam is focused to a spot with the tube unblocked and the tube is then operated without changing the focusing field current, the trace is sharp at the beginning of the sweep but the trace widens almost uniformly during an interval of two microseconds. The term defocusing has been applied to this phenomenon. The width of the trace normally remains constant for the remainder of the sweep after this two microsecond interval, although the width would occasionally decrease slightly after a maximum width had been reached. Usually the focus was sharp at the exact beginning of the sweep but in certain instances the

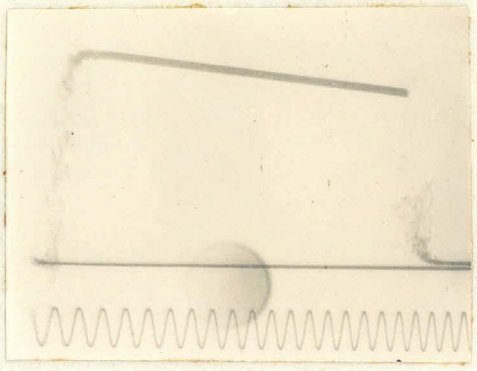

Figure 12
Surge Oscillogram
1 megacycle timing wave

Figure 13
Transient gas focusing
Interval of defocusing 2 microseconds

beginning of the sweep might be out of focus and the sharpest focus would then occur during the interval of defocusing. This interval of defocusing is independent of sweep speed; in fact, it is independent of every conceivable variable that was checked during the three years of research on the problem.

Actually, the term overfocusing might be more descriptive of the phenomenon termed defocusing. In all cases the beam can be focused sharply by reducing the current in the focusing field from the value required for focus of the spot when the beam is not blocked. This behavior suggests the possibility of transient gas focusing which is not present during steady state conditions.

The correlation between defocusing and the use of fore-concentration was evident at almost the same time that the defocusing itself was discovered. The reason for such a correlation was not understood, however, until the various factors affecting the distribution and quantity of stray electrons inside the tube had been investigated. Further basis for the misleading belief that fore-concentration is directly responsible for defocusing was furnished by the accidental discovery that reversing the direction of the current in the fore-concentration field reduced the magnitude of the defocusing. Later tests failed to verify this reduction of defocusing and this solitary example of reduced defocusing can probably be explained by some change in the mechanical alignment of the cathode assembly while reversing the leads to the fore-concentration field. Very slight changes in the alignment of the cathode cause relatively great changes in the beam current. This behavior will be described in detail in a later discussion of beam efficiency.

It is possible to obtain an electron image of the cathode surface by adjusting the strength of the fore-concentration field. Examination

of the electron density distribution in the beam in this way shows that most of the electrons in the cathode beam originate at the bottom of a crater which forms on the surface of the cathode. An early observation showed that moving the image of the bottom of the cathode crater out of the beam also reduced the defocusing.

All of these first observations can now be explained by the theory of a correlation between defocusing and the presence of a large number of stray electrons, since the changes involved invariably reduced the number of stray electrons by reducing the beam current.

The first intimation that defocusing is related to the presence of a large number of stray electrons was given by the observation that defocusing is much greater than usual when the use of fore-concentration causes a tremendous reduction in the deflection by the electrostatic bias voltage applied to the sweep plates. Further investigation revealed that the current between the plates shows a saturation effect as an isolated voltage across the plates is increased, indicating that the current is being limited by the number of stray electrons available. The saturation current under the same voltage conditions was tripled when the beam current was nearly tripled by using fore-concentration. If the center tap of the voltage across the sweep plates was grounded - normal operating condition - the stray current without fore-concentration was increased somewhat and the use of fore-concentration then caused the stray electron current to increase by a factor of eight. The maximum measured stray current caused a reduction of the bias voltage of 10% and the reduced deflection of the beam when fore-concentration was used verified this result experimentally. The reduction of deflection involved was much less than during the previous experiment when the correlation between defocusing and reduced deflection with fore-concentration was first noted.

Grounding the middle sphere of the trip gap reduces the defocusing. This connection requires the application of the tripping impulse for surge recording to one of the outside spheres. Some inconvenience is caused by the necessity of changing the connection for surges of different polarity but the system has been quite practical. The possibility that the entire blocking system might be "floating" at some potential above ground was considered but discarded after tests showed that the distortion produced when the blocking plates are raised to some potential above ground is quite odd shaped and can never be focused sharply, while photographs made with the sweep disconnected show that the defocused beam is circular in shape.

Encouraging results were obtained by applying 90 volts to the blocking plates. A slight deflection was produced and the focus was changed radially by approximately the proper amount and in the correct direction to explain defocusing. Paradoxically, grounding the middle sphere increased the focusing effect, in contrast to the opposite behavior in the transient or true defocusing case. However, when the vacuum was improved by using a liquid air vapor trap, tests failed to show any focus effect with 90 volts applied to the blocking plates, although defocusing was still present during normal operation of the oscillograph. Further tests without liquid air in the trap repeated the original results. The polarity of the voltage applied to the blocking plates with respect to ground causes different visible transient effects but the steady state results are similar, although not exactly the same. No change in the deflection sensitivity is apparent when the focus is changed by voltage on the blocking plates.

During tests of beam current and stray electron currents as a function of pressure in the tube, a focusing effect was noted when voltage

was applied to the sweep or deflection plates. This focusing effect is similar to that observed when low voltage is applied to the blocking plates. A saturation effect can be noted, i.e., no additional focusing effect is observed as the voltage is increased beyond 200 volts. Voltage was applied to the deflection plates with the beam unfocused; the beam was then focused to a point and the beam blocked and swept; the result was a broad trace. The beam was focused to a point with no deflection voltage; then the same deflection voltage as used in the previous test was applied and the spot became over-focused; the result was a sharp trace when the beam was blocked and swept. These tests seemed to prove that the focusing effect observed in the static case when voltage is applied and stray electrons are present cannot explain the defocusing when the beam is blocked and then swept.

Additional check of the theory that defocusing might be caused by the spark gap voltage across the blocking plates was made by connecting batteries in series with the leads from the trip gap to the blocking plates. The gap voltage had been measured with the oscillograph. Visual observation indicated a total gap voltage of about 100 volts; photographic measurement gave a value nearer 50 volts for the total gap voltage. Both 22½ volt and 45 volt batteries were connected on each side of the gap, in correct and incorrect polarity for compensating the gap voltage, with and without middle sphere grounded, yet no observable change in the defocusing could be noted. Such definite negative results seem indisputable.

A comparison of the defocusing when either single pair of blocking plates were used alone or when both pairs of plates were used, did not furnish any conclusive data. An attempt was made to observe the trace when the beam was swept with the blocking plates disconnected. The fast sweep was obscured by the slower return sweep. The return sweep appeared to be focused sharply. Results were again inconclusive. Defocusing

definitely occurs and can be photographed with the sweep plates disconnected, but with regular unblocking taking place. This result proves that the sweep transient is not responsible, although it cannot be said that the presence of the sweep and/or deflection plates does not influence the phenomenon. Defocusing also occurs when the deflection plates are substituted for the regular sweep plates.

There is no change in the deflection sensitivity of the beam when the beam becomes defocused. The deflection sensitivity was measured for beams of different energies requiring focusing field currents less than, and greater than, the focusing field currents used for focusing a defocused beam and an unblocked beam. There should have been a deflection variation of one-fifth of an inch during the defocusing interval with 500 volts on the deflection plates if the effect were due to a change in the energy of the electrons in the beam above the deflection plates, but the trace was a straight line. Defocusing is identical when photographed with the electrons hitting an insulating gelatine emulsion, or observed visually as the electrons strike a fluorescent coating on an aluminum plate. Any explanation based on deceleration of the beam by an electron "film" at the bottom of the tube can therefore be eliminated.

The fact that the magnitude of the focus effect is so great - in rare cases a sharp trace with a defocused beam has been obtained with zero magnetic focusing field - and the fact that grounding the middle sphere of the trip gap influences the effect, support a belief that the transient focusing occurs in the upper region of the tube, probably in the vicinity of the blocking plates. This part of the tube is a region of relatively high gas pressure. Additional evidence is contributed by the behavior of the beam when the trip gap is not symmetrical with respect to ground. After the trip lead has been moved from the middle sphere to

an outside sphere, the beam cannot be focused at all if the middle sphere is ungrounded; the trace is a smear for any value of focus field current. Grounding the middle sphere through a resistance of several hundred ohms allows most of the trace to be focused, leaving a "fan" at the beginning of the sweep which cannot be focused under any conditions. The trace has some smear at the beginning of sweep when the vacuum is poor if the trip lead is connected to the middle sphere.

A series of tests with various trip gap connections led to the following conclusions: if vacuum is good, either due to continuous pumping when the relative humidity of the atmosphere is low so that film and tube become dry, or by the use of a liquid air trap, there is little smearing of the trace if the trip gap is completely floating, i.e., entirely disconnected from the trip lead. If the trip lead is connected to any part of the circuit, it tends to maintain the circuit at the condition before tripping; for example, if the trip lead is connected to the middle sphere but floating, it is essentially at ground potential and the trace is satisfactory with a good vacuum. But, if the trip lead is connected to the middle sphere and to the tap between a pair of unequal resistors across the complete gap, or if the trip lead is connected to an outside sphere, the lead effectively prevents the blocking system from being symmetrical with respect to ground and the result is a smeared trace. The trace is satisfactory, however, if the middle sphere is grounded through a 100 ohm resistor, regardless of the state of the vacuum, and the trip lead can be connected to either the middle sphere or to an outside sphere.

One other observation should be mentioned. A temporary, visibly radial change in the size of the focused spot can be observed occasionally as the electrostatic bias voltage is applied to the sweep plates. No investigation was made of the phenomenon, as its occurrence was quite rare.

The phenomenon may be explained by a transient gas focusing caused by moving the electron beam into a new path, destroying the equilibrium between the positive and negative space charges in the region near the cathode beam.

One factor remained important throughout the entire investigation. Any increase in the number of stray electrons increases the defocusing effect if other factors remain constant. Poor vacuum invariably causes defocusing, but no difference can be detected between a poor vacuum due to water vapor within the tube or a dry tube with the air pressure equal to the partial pressure of the water vapor in the first case. Stray electrons increase as the beam current increases, regardless of the cause of the increased beam current, but not necessarily in proportion to it. This behavior explains the correlation between defocusing and fore-concentration. No definite relation could be discovered between defocusing and the number of stray electrons present at different locations within the tube. In fact, defocusing was known to occur when stray electrons were less numerous than during a previous test in which defocusing did not occur.

Gas focusing alone cannot be considered an adequate explanation. Gas focusing would predict an unfocused beam at the beginning of sweep, with the rest of the trace focused after ionization had occurred, due to the release of the beam. This behavior does not occur. Some slight gas focusing was observed in the steady state with the beam not blocked when the beam current was exceptionally high, i.e., greater than 60 microamperes. As evidence for the existence of such gas focusing, the trace was underfocused at the start of the sweep; passed through a point focus; then became badly defocused.

A complete explanation which satisfies all of the observations

relating to defocusing would be quite complex. A simplified explanation can be based on a transient gas focusing. The interval of defocusing is the time required for the formation of a positive ion space charge. Normally, the ions maintain the gas focusing for a period not longer than the persistence of vision. The duration of defocusing with the beam stationary was checked by unblocking the beam by shorting the blocking plates after the blocking voltage had been disconnected. The sweep impulse was not applied to the sweep plates during this test. The eye perceived an overfocused spot which changed instantly to the point focus, characteristic of the focused beam with the beam not blocked. Perhaps the defocusing persists as long as the beam is moving into a region of unionized gas molecules. At any rate, some relation between the mobilities of the ions and the stray electrons created when the gas molecules become ionized allows the neutralization of the space charge causing gas focusing when equilibrium has been established, but permits the occurrence of a transient gas focusing. The number of positive ions would increase as stray electrons increased, but would not necessarily be in the form of a space charge which would cause gas focusing.

Such an explanation does not offer a good correlation with the behavior when the middle sphere of the trip gap is grounded. But most other observations can be explained, at least partially, by the hypothesis.

The uniformly radial focusing effect of an electrostatic field may be explained by a steady state gas focusing produced by the effect of field on the motion of the positive ions or the stray electrons, or both, preventing the normal equilibrium from being established under steady state conditions. It is known that electric fields affect the operation of hot-cathode, gas-focused cathode-ray tubes. J. B. Johnson[10] mentions a momentary "pause" in the trace of a sine wave in a tube using gas focusing,

caused by the neutralization of weak electric fields by the space charge. This "pause" when the deflecting field was weak was never observed with this oscillograph.

At the present time there is no information to prove that this defocusing behavior is not limited to this particular oscillograph. However, it is likely that the phenomena have been observed by others.

Fortunately, defocusing can be minimized by using a low beam-current for the sweep speeds coinciding with the interval of defocusing. The trace with an unconcentrated beam is invariably sharper and preferable to a trace using fore-concentration. Fore-concentration is primarily useful for increasing the visible intensity of the oscillogram when observing with a fluorescent screen, or for photography with sweep speeds approaching the writing speed limit. In the latter case, the interval of defocusing is very long compared to the period of sweep and defocusing is not objectionable. Good oscillograms are therefore possible throughout the entire operating range of the oscillograph, if careful technique is employed.

A third form of beam distortion was observed occasionally when an abnormally large amount of water vapor was present in the vacuum system. The observed effect was a series of unfocused beads connected by a sharply focused trace. This bead distortion is illustrated by Figure 14. (The effect became familiarly known as the gopher snake because its appearance resembles a well-fed snake of that species).

Bead distortion always occurs simultaneously with an abrupt decrease in the discharge-current, other factors remaining unchanged. This decrease in discharge-current represents a discontinuity in the discharge-current - discharge pressure curve. The air pressure in the discharge tube

Figure 14
Bead Distortion
Time scale microseconds

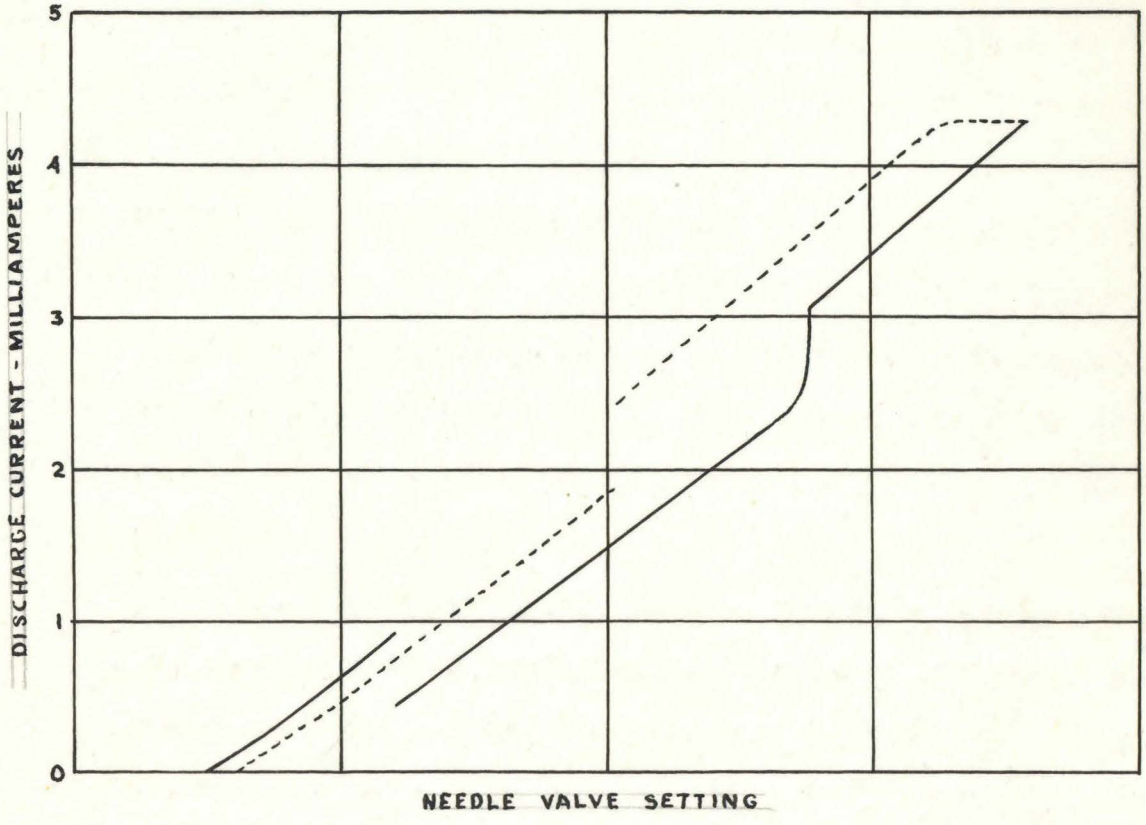

FIGURE 15

was not known, but it is not unreasonable to believe that a continuous change in the setting of the needle valve leak gives a continuous variation of the pressure within the discharge tube. Figure 15 shows the relation between discharge-current and needle valve setting during the period when bead distortion exists. Discharge-current begins and increases to 1.0 milliamperes as the needle valve is opened. The oscillograph trace is sharp throughout this first region. No defocusing is apparent. Then the discharge-current will drop suddenly to 0.5 milliamperes and beads will appear in the trace occasionally. With the beam unblocked, the beads appear as a "halo" around the focused spot. The unfocused spot is not as sharply defined as it would be with a normal discharge. Usually, the discharge-current creeps upward to a normal value and the beads disappear if the needle valve leak is increased until the discharge-current becomes 2.5 milliamperes. This is illustrated by the vertical solid line in Figure 15. Occasionally, however, the change from a low discharge-current to a higher discharge-current is discontinuous.

Decreasing the needle valve leak causes the discharge-current to decrease to a value somewhat less than 2.5 milliamperes; then a discontinuous drop of approximately 0.5 milliamperes occurs and the discharge-current remains low until the discharge disappears, due to an insufficient air leak. The behavior as the needle valve leak is decreased is shown by the dotted line in Figure 15.

The duration of the individual beads is invariable, although the frequency of occurrence of the beads increases as the discharge-current is increased from 0.5 to 2.5 milliamperes by opening the needle valve leak. Figure 14 shows three beads during an interval of 200 microseconds. The frequency of occurrence is seldom greater than this value. On one occasion the frequency of occurrence was approximately once in 500 to 1000 micro-

seconds with a discharge-current of 0.5 milliamperes; increasing the discharge-current to 0.8 milliamperes increased the frequency of occurrence and the beads appeared consistently in semi-connected pairs. Further increase of the discharge-current to 1.0 milliamperes caused semi-connected triplets separated by a relatively sharp trace. These multiple beads are not the usual phenomenon, however.

Bead distortion and the region of low discharge-current disappear immediately when a liquid air trap is used if the water vapor within the tube has been introduced by new films. But continuous pumping for several days was required to reduce bead distortion when the water vapor was introduced by a wet towel wrapped around the needle valve leak.

Two independent checks proved that the beads must be a focus effect and cannot be caused by periodic changes of acceleration voltage due to a variable drop across the limiting resistance in the lead to the cathode, as the discharge-current fluctuates between the two regions of current indicated by Figure 15. Changing the value of the limiting resistance produced no observable difference in the size, shape, or the frequency of occurrence of the beads. Voltage was applied to the deflection plates while bead distortion was occurring. No change in the deflection sensitivity of the beam occurred when the beads appeared, a further indication that the effect is caused by a focus phenomenon. An interesting but uncorrelated observation is that no change in the voltage across the trip gap occurs when a bead appears. This observation was made with the blocking gap connected to the deflection plates.

There is no obvious explanation for the simultaneous occurrence of a periodic focus change and the discontinuous behavior of the discharge-current. M. von Ardenne[11] describes an anomaly termed 'Ionenschwingungen' which gave a periodic focus variation, but the cathode-ray tube was a

sealed glass, hot-cathode, gas-focused tube. Some data by Güntherschulze quoted by Loeb[6] show a non linear variation of the cathode fall of potential as the percentage of hydrogen in a mixture of mercury and hydrogen is varied from 0 to 100% hydrogen. A similar behavior might explain the discontinuous behavior of the discharge-current in a mixture of air and water vapor. In discussing the anomalous behavior of discharges in a mixture of gases, Loeb comments, "..... speculation is futile."

ANOMALIES

Several interesting anomalies occurred. Most of them were unimportant, but some were sufficiently curious to be worthy of mention.

At one time a faint glow appeared on the fluorescent screen when the beam was biased to the left of the screen and blocked. This ghost beam behaved quite normally in a magnetic field, moving in the legitimate direction. But as the electrostatic bias was decreased and the beam returned to the center of the screen, although blocked and not visible, the ghost beam disappeared in the opposite direction. The ghost beam is readily explained by a few stray electrons of high energy which passed through the blocking windows and between the left sweep plate and the brass wall of the oscillograph tube. The electrostatic field between the plate and the wall of the tube has a direction and magnitude which deflected the stray beam back toward the screen. The ghost beam disappeared when the cathode then in use was replaced.

Another rather amazing effect was observed during some tests with a single sheet of process film in the oscillograph. Figure 16 is a photograph made by unblocking the unconcentrated beam with sweep No. 6, the slowest available sweep speed, disconnected from the sweep plates. The beam is split into two sections which have separated slightly. The

Figure 16

Figure 17

Figure 18

degree of "splitting" of the unfocused beam decreased as the unblocked interval was shortened by selecting faster sweep speeds. When first unblocked by removing the voltage supply, the beam had a normal circular shape with a faint line through the beam as in Figure 18. The beam would then fly apart and gradually attain an appearance similar to Figure 17. The figures have been drawn to the same scale as the photograph. Lack of additional film in the camera prevented taking other photographs of the phenomenon.

The film was then removed. The cathode was removed at the same time and inspected. It had a normal appearance with a barely formed crater. The same cathode was re-installed without particular care to obtain the previous alignment. (This test occurred before the significance of cathode position was discovered). The beam was at first satisfactory, but still had the shadow line shown in Figure 18. An hour later, with the beam off during the interval, the split beam returned. The air leak at the needle valve was accidentally cut off and the beam became circular again, with the shadow position changed somewhat. As yet, no fore-concentration had been used. A weak fore-concentration field widened the separation of the beam at the shadow. The position of the shadow did not change as the electron image of the cathode was moved to different regions of the beam by changing the position of the fore-concentration field. One critical value of fore-concentration field-current and position caused the beam to fly apart. The pattern differed from Figure 17. This difference was expected, since the position of the shadow had changed as noted above. The split beam could not be focused to a point, and the beam did not appear split if overfocused. Eventually, the phenomenon disappeared.

It is difficult to attempt to explain a phenomenon at a later date when new factors are discovered, but the behavior as the original cathode

aged (a new crater would undoubtedly be formed after the cathode was re-installed, and the effect would be identical to the installation of a new cathode) could have been caused by the first sudden decrease of the beam-current making fore-concentration necessary to maintain the intensity of the beam. A minute obstruction, which was eventually burned away by the beam, must have caused the observed shadow in the beam. Probably the obstruction was located at the limiting aperture below the anode window, as its position changed when the needle valve leak was accidentally cut off and disappeared soon after fore-concentration was used.

On one occasion, the unfocused beam appeared as two distinct concentric beams, one larger than the other. This beam could be focused to a spot with a surrounding underfocused or overfocused beam by focus field-current values of 0.290 amperes and 0.315 amperes respectively. The higher current was the current normally required for focusing. An attempt to measure the deflection sensitivity of the double beam failed because the dual character of the beam disappeared when deflection voltage was applied and slowly returned when the deflection voltage was removed. The double beam did not seem to be affected if blocking voltage was applied and immediately removed. Continued blocking of the beam caused the beam to lose its dual character although the double beam returned slowly if the beam was left unblocked.

A list of the various anomalies, their cause and correction, if known, is given in Table II.

TABLE II

LIST OF ANOMALIES

ANOMALY	CAUSE	CORRECTION
Bead Distortion - Periodic Overfocusing Phenomenon	Water Vapor in Vacuum System	Removal of Water Vapor
Stray beam with blocking voltage applied	Old Cathode	New Cathode
Beam split and separated	Obstruction between anode and blocking chamber	Obstruction disappeared
Two concentric beams	Unknown	Occurred only once. Eliminated by electro-static field
Cyclic variations of Beam Efficiency	See discussion in BEAM STUDIES	Aging a new cathode

The use of a cold-cathode oscillograph as an electron microscope has considerable practical value as well as theoretical interest. Busch[12] has shown that a short axial focusing coil acts like an optical lens. Two axial magnetic fields are available on the oscillograph. One is normally used to focus the discharge on the anode window and increase the beam current; it is known as the fore-concentration field. The other is used to focus the cathode-beam to a spot on the fluorescent screen and will be referred to as the focus field. These fields are given by the leakage flux from the air gap in an iron case with axial symmetry. The analogy to a thin lens is therefore quite good.

An image of the cathode surface is formed on the fluorescent screen if the fore-concentration field is adjusted to a value somewhat less than that required for maximum increase of the beam current. The field of the image is limited by an aperture located between the anode and the blocking system. This aperture is required for operation of the tube as an oscillograph. With zero focus field current, the image is about 1.2 cm. in diameter and represents a magnification of approximately 50 diameters. A focus field current of 0.30 amperes is normally required to give a point focus, or image of the anode window at the fluorescent screen. The distance from the anode window to the focusing field is 45 cm. and the distance from the focusing field to the fluorescent screen is 55 cm. Increasing the focusing field current from 0.30 amperes to 0.35 amperes decreases the image distance from 55 cm. to 35 cm. If full battery voltage (6 volts) is applied to the focus field, the field current will be 0.64 amperes. This value of focus field current forms an image of the anode window well above the fluorescent screen, and a spot twice as large as the

unfocused spot appears on the fluorescent screen. Since the electrons from a particular point on the cathode surface are traveling in paths essentially parallel, because of the small diameter of the anode window, the focus field produces little change in the focus of the electron image of the cathode surface, and an enlarged but inverted image of the cathode appears on the fluorescent screen. Additional voltage can be applied to the focus field, increasing the magnification to approximately 500 diameters, but sharpness of detail is sacrificed. Some rotation of the image is produced by both axial fields. The rotation seldom exceeds 90 degrees.

This arrangement of a pinhole aperture and two magnetic "converging lenses", one to control the focus of the image and the other to vary the magnification, differs from the electron microscopes described by Zworykin[13], Ruska[14], Myers[7], and Maloff and Epstein[8], but the design is quite effective. Several optical analogies possible with the system are illustrated by Figure 19. Figure 19c is the simplest analogy, and has been checked with a flashlight, a pinhole, and a camera lens. The image from such an arrangement is, of course, poor, due to the large magnification from a pinhole lens.

It is possible to examine the electron image of the cathode surface and observe the changes which occur as the cathode is used. This fact was useful in observing the formation of a crater in the end of the cathode, and showed definitely that the sudden decrease in beam efficiency after a cathode has been in use for approximately 5 minutes coincides with the formation of such a crater. (See Figure 23 for curves of beam current as a function of cathode age). The image of a new cathode shows that the source of the electrons is influenced by lathe tool marks and similar surface irregularities. The action of positive ions striking the cathode surface soon removes these irregularities. A crescent-shaped bright spot appears. This spot increases in areaand forms a semi-circle with a bright

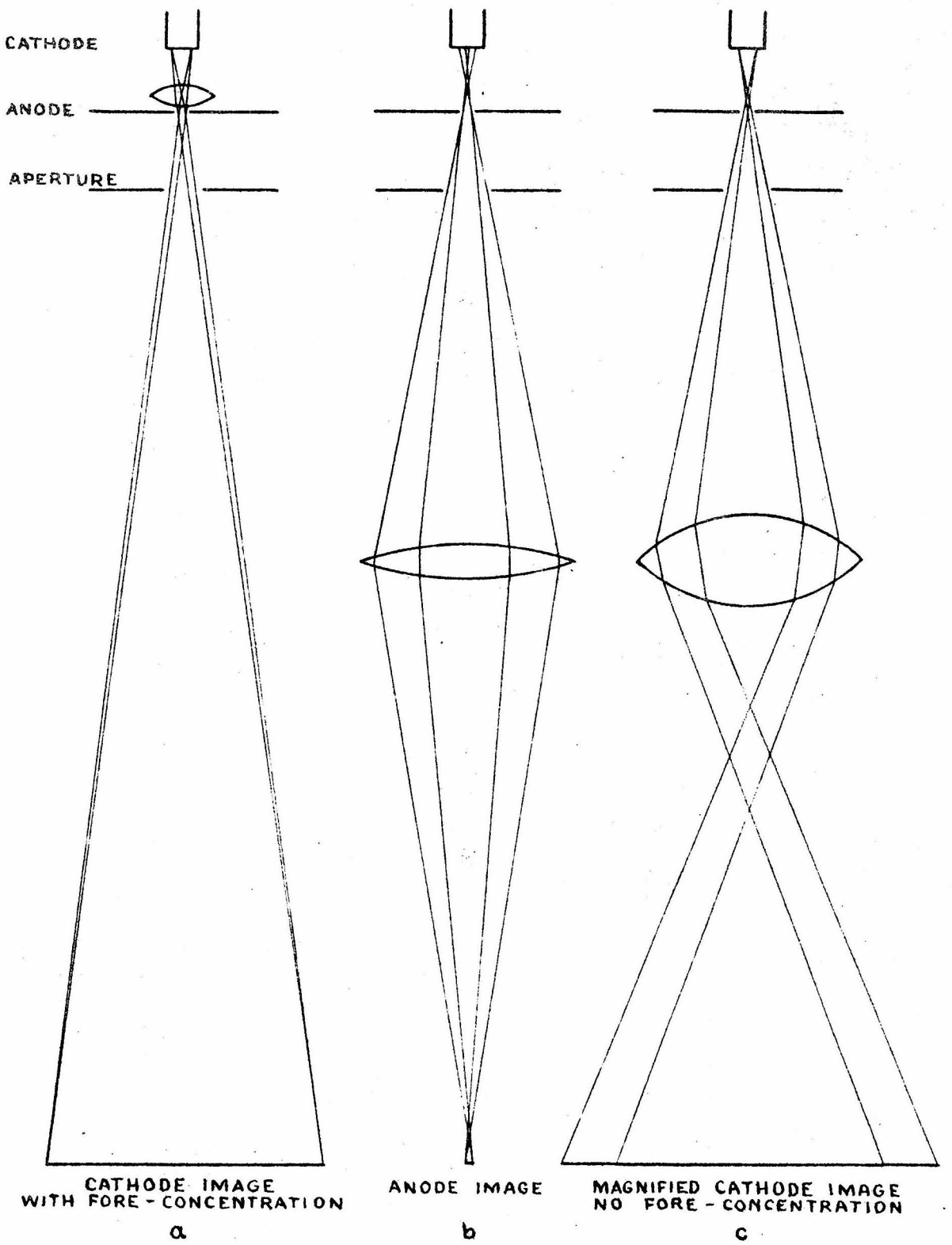

FIGURE 19 OPTICAL ANALOGIES FOR THE OSCILLOGRAPH

spot in the middle of the arc, like a marble resting in the bottom of a bowl. The arc gradually becomes a complete ring, and the bright spot moves to the center of the ring with a relatively dark area between the central spot and the outer ring. Very old craters may show a second larger and weaker ring. The size of the ring varies with the age and size of the crater, of course.

Experience has shown that fore-concentration is not as valuable as might be expected from the increased beam-current which it makes available. The trace cannot be focused as sharply as the trace without fore-concentration; as a result, the width of the trace increases and the apparent blackness of the trace is not increased. Difficulties due to transient gas focusing are increased by the increased beam-current. For these reasons, fore-concentration has not proved satisfactory for photographic recording except at the extremely high sweep speeds. Fore-concentration is quite valuable for visual observations, however, as the brilliance of the trace on the fluorescent screen is increased considerably by the increased beam-current.

Fore-concentration increases the beam-current to a value six times as great as the value without fore-concentration if the total discharge is small, i.e., 0.5 milliamperes. The efficiency of fore-concentration decreases as the total discharge current is increased, but the beam-current increases until an optimum value of total discharge-current is reached. Further increase of the total discharge current causes only a slight reduction of the beam-current if no fore-concentration field is used, but the efficiency of fore-concentration becomes quite low after the optimum value of total discharge current is exceeded. Note the curves of beam-current as a function of fore-concentration field-current for discharge-

currents of 4.0 and 5.0 milliamperes (Figure 20). The values of beam-current without fore-concentration, and beam-current when the fore-concentration field current is adjusted to its optimum value, have been replotted in Figure 21 as a function of total discharge-current.

Maximum beam-current occurs when the fore-concentration field-current is adjusted to a value somewhat higher than the value required for an electron image of the cathode surface at the fluorescent screen. If there were no limiting aperture below the anode, a maximum should occur when the discharge is focused on the anode window. The presence of the aperture requires that the image of the cathode be focused at a plane between the anode window and the aperture. Influence of the magnetic field upon the nature of the discharge may affect the adjustment for maximum beam-current, particularly when the total discharge-current is high; although the fact that the maximum beam-current occurred when the overfocused image of the bottom of the cathode crater just filled the field limited by the aperture, indicates that the geometrical factors control the maximum beam-current for any constant, low value of discharge-current.

A beam-current as high as 8% of the total discharge-current has been obtained with low discharge-current (0.3 milliamperes). Beam efficiencies of 5% were obtained consistently with discharge-current values of 0.5 milliamperes.

Discharge-current increases as the fore-concentration field strength is increased if no adjustment of the needle valve leak is made to reduce the pressure in the discharge tube. This current increase continues beyond the value of fore-concentration field-current which gives the maximum beam-current. As an example, the total discharge-current was adjusted to 1.0 milliampere with zero fore-concentration field-current. The beam-

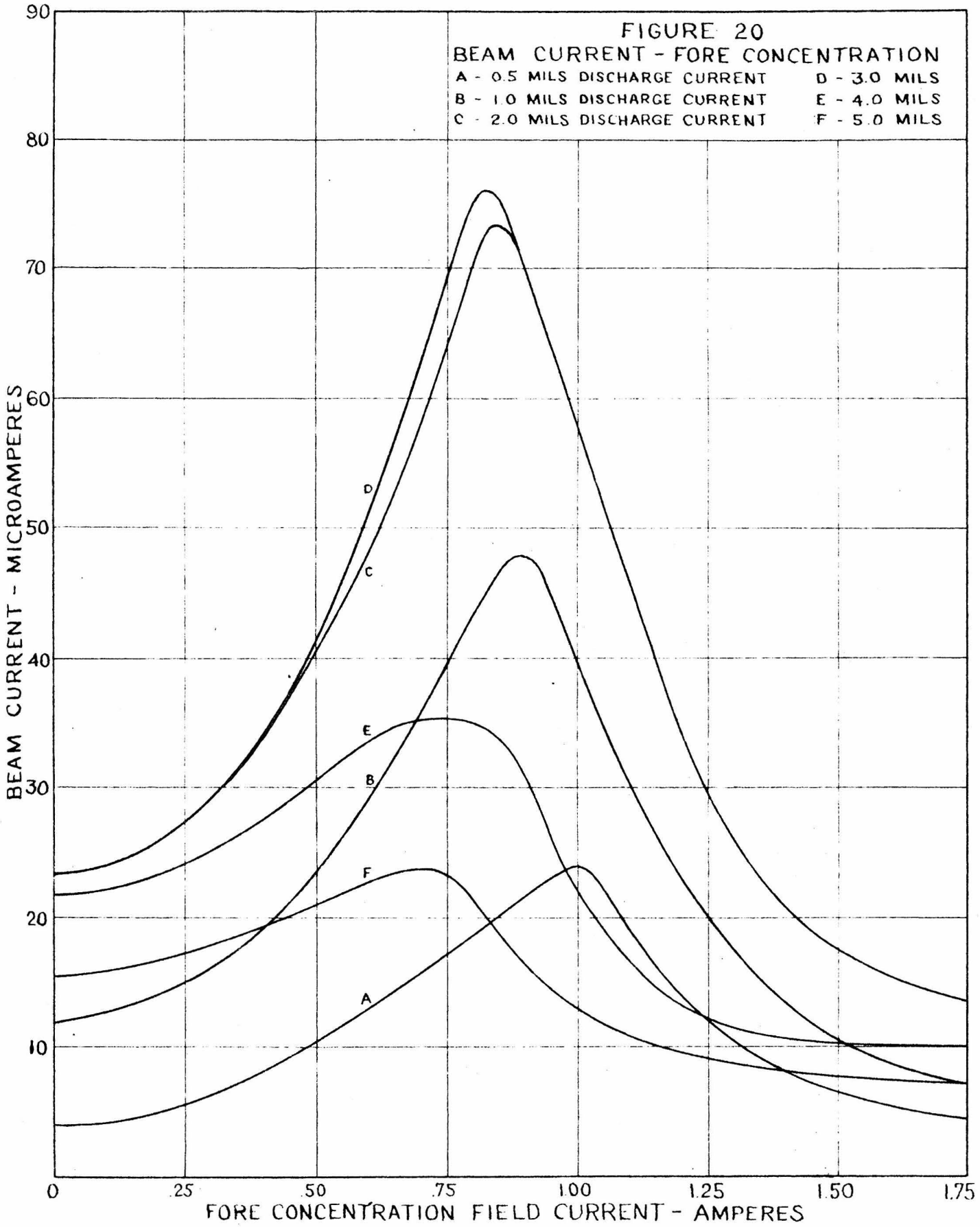
FIGURE 20
BEAM CURRENT - FORE CONCENTRATION
A - 0.5 MILS DISCHARGE CURRENT
B - 1.0 MILS DISCHARGE CURRENT
C - 2.0 MILS DISCHARGE CURRENT
D - 3.0 MILS
E - 4.0 MILS
F - 5.0 MILS
BEAM CURRENT - MICROAMPERES
90
80
70
60
50
40
30
20
10
0
.25
.50
.75
1.00
1.25
1.50
1.75
FORE CONCENTRATION FIELD CURRENT - AMPERES
D
C
E
B
F
A

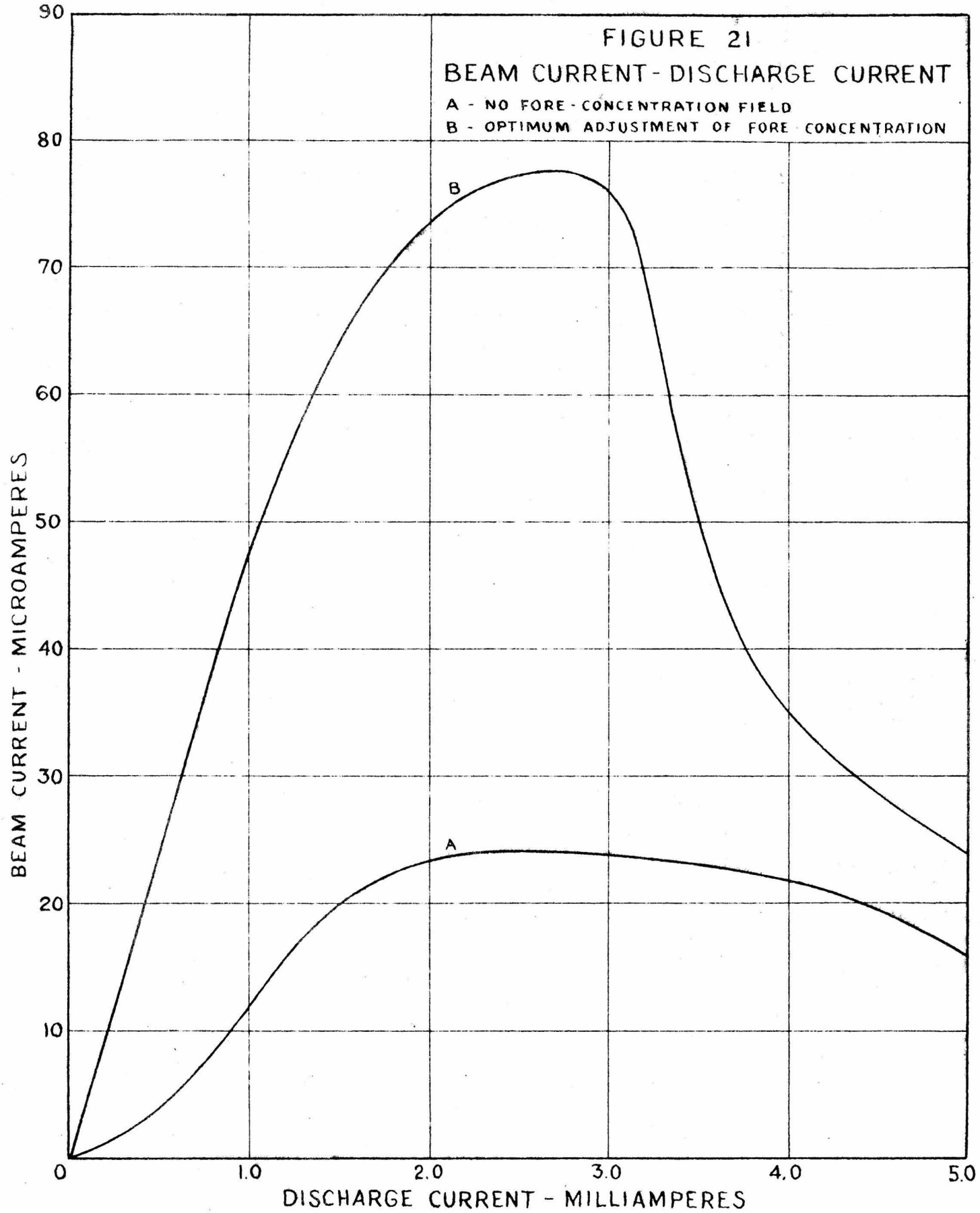
FIGURE 21
BEAM CURRENT - DISCHARGE CURRENT
A - NO FORE - CONCENTRATION FIELD
B - OPTIMUM ADJUSTMENT OF FORE CONCENTRATION
B
A
90
80
70
60
50
40
30
20
10
0
1.0
2.0
3.0
4.0
5.0
BEAM CURRENT - MICROAMPERES
DISCHARGE CURRENT - MILLIAMPERES

TABLE III

FORE-CONCENTRATION FIELD-CURRENT VALUES FOR

IMAGE OF CATHODE AND MAXIMUM BEAM-CURRENT

Total Discharge Current. Milliamperes	0.5	1.0	2.0	3.0	4.0	5.0
Beam Current with Zero Fore-concentration Field. Microamperes	4	12	23	23	22	16
Maximum Beam Current. Microamperes	24	48	73	76	35	24
Fore-concentration Field-Current for Maximum Beam-Current. Amperes	1.00	.90	.85	.80	.75	.70
Fore-concentration Field-Current for Cathode Image. Amperes	.85	.75	.72	.70	.65	.65

current under these conditions was 10 microamperes. When the current in the fore-concentration field was increased to 1.0 ampere, the total discharge-current increased to 2.0 milliamperes and the beam-current to 60 microamperes. Increasing the fore-concentration field-current to 1.5 amperes increased the total discharge-current to nearly 3 milliamperes and reduced the beam-current to 12 microamperes. This behavior of the total discharge-current is readily explained by the action of an axial magnetic field on a glow discharge.

The data plotted in Figure 20 were obtained by readjusting the needle valve leak so that total discharge-current was constant at the value shown for each curve. No adjustment of the accelerating voltage was made; each curve in Figure 20 represents a constant voltage but the voltages for the different curves differ by the drop across the limiting resistor. A well-aged cathode was used in order to avoid fluctuations of beam efficiency (see Figure 23), but some variation did occur during the test, which required more than one hour, and it was not always possible to repeat values. For this reason, Figures 20 and 21 are merely representative data, and certain unavoidable but relatively unimportant variables are included. A list of additional data not shown by the curves is included in Table III following Figure 21.

BEAM STUDIES

Beam efficiency is influenced by a number of other factors as well as by concentration of the discharge with an axial magnetic field. The effect of water vapor within the tube was mentioned in the discussion of transient gas focusing and other forms of beam distortion. The increased number of stray electrons which is always associated with a poor vacuum must be accompanied by a decrease in the beam-current, since the stray

electrons are formed by the collision or interaction between gas molecules and the electrons in the beam. Figure 22 illustrates typical data which show the improvement in the beam-current as water vapor is removed from the system by a liquid air trap. When liquid air was first added to the trap, the beam-current was 12 microamperes, and the stray electron-current at the right sweep plate, measured with the positive terminal of a 90-volt battery connected to the sweep plate and a microammeter in series with the lead to ground, was 18 microamperes. Beam-current increased to 30 microamperes and the stray electron-current decreased to $4\frac{1}{2}$ microamperes over a period of three hours, and after that time remained steady. The length of time required for complete removal of water vapor from the system was not always as great as three hours. In some cases improvement was almost instantaneous.

Stray electrons increase more rapidly than the beam-current when the beam-current is increased by a fore-concentration field if the vacuum is poor. But the ratio of beam-current to the stray electron-current at the right sweep plate increases as beam-current is increased when the oscillograph is free of water vapor and the air pressure is 2×10^{-4} mm. of mercury, probably because the leak is decreased slightly to maintain constant total discharge-current. Such variations are second order effects, however, and in general the number of stray electrons is proportional to the beam-current if pressure conditions within the tube are not varied.

The distribution of stray electrons in the various parts of the oscillograph varied at different times, and this variation could not always be correlated with variations of gas pressure at different parts of the tube. Apparently the distribution of stray electrons is also affected by the intensity of the current in the beam, but no definite relation was determined.

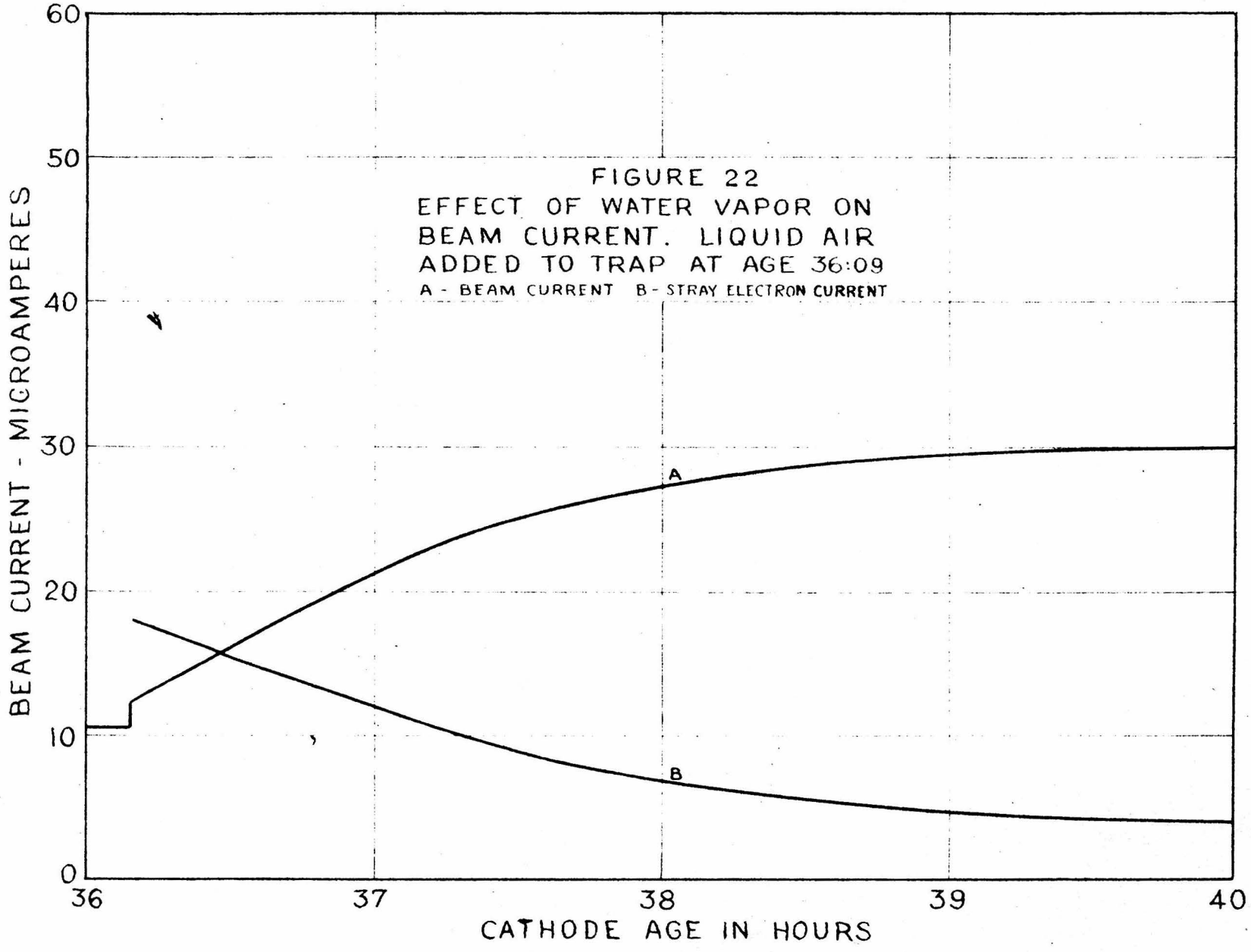

FIGURE 22
EFFECT OF WATER VAPOR ON BEAM CURRENT. LIQUID AIR ADDED TO TRAP AT AGE 36:09
A - BEAM CURRENT B - STRAY ELECTRON CURRENT

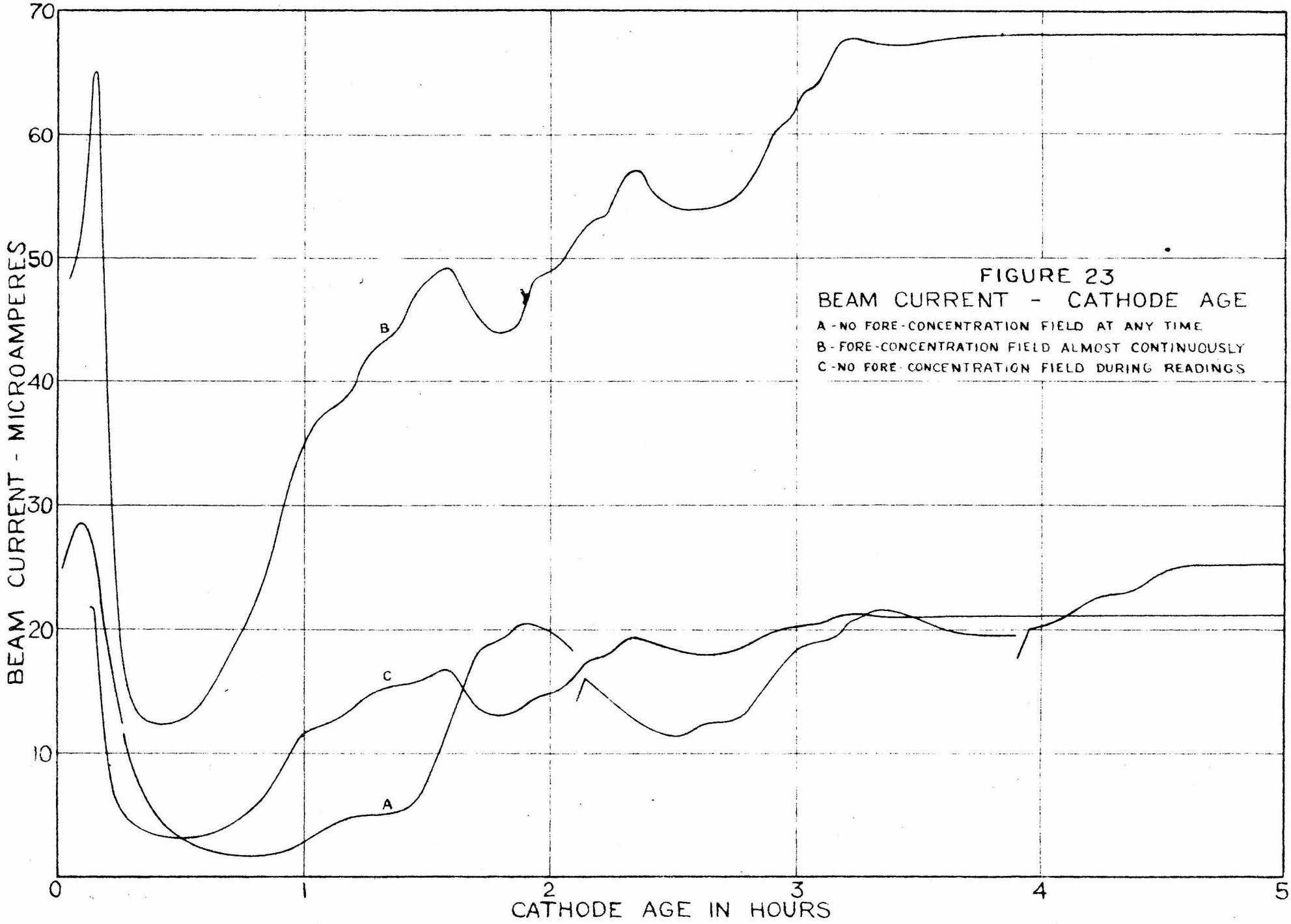
70
60
50
40
30
20
10
0
1
2
3
4
5
BEAM CURRENT - MICROAMPERES
CATHODE AGE IN HOURS
A
B
C
FIGURE 23
BEAM CURRENT - CATHODE AGE
A - NO FORE-CONCENTRATION FIELD AT ANY TIME
B - FORE-CONCENTRATION FIELD ALMOST CONTINUOUSLY
C - NO FORE-CONCENTRATION FIELD DURING READINGS

An auxilliary leak valve in the lead between the oscillograph and the vapor pumps allowed tests to be made at pressures higher than the normal operating pressure of 2×10^{-4} mm. of mercury with the needle valve leak in the discharge tube the major source of gas in the tube. The first visible change in the appearance of the beam occurred at a pressure of 5×10^{-3} mm; stray electron illumination of the background increased noticeably and the edge of the beam became less sharply defined. At 1×10^{-2} mm. air pressure the tube was still operative, but transient defocusing was quite bad, and the sweep voltage flashed over to ground frequently. This behavior was identical to the operation of the tube with water vapor present at about the same pressure (1×10^{-2} mm.) and a much lower partial pressure of the air itself.

Cathode surface conditions are a second factor which influences beam efficiency. A cathode which has not been in operation for some time gradually regains its efficiency if operated continuously. The loss of efficiency depends on the length of time the cathode has been inoperative. The discontinuities in curve A, Figure 23, represent efficiency changes caused by removing the accelerating voltage for short intervals to determine whether the cyclic variations of efficiency were caused by continuous operation. The break at time 15 minutes was not longer than 5 minutes in duration, while the breaks at 2 hours and 4 hours lasted approximately 30 minutes each. The water vapor trap was filled with liquid air continuously during these tests. On several other occasions, after the tube had been inoperative over night, voltage was applied intermittently until no further increase of beam-current or decrease of stray electron-current was observed, to assure that the tube was free of water vapor. Then voltage was applied continuously, and the beam-current and stray

electron-current both increased during an interval of one hour. The beam-current nearly doubled during the interval, and then became steady at the value of beam-current observed during the tests made on the previous day. This behavior varied with different cathodes, but does indicate a relation between beam efficiency and cathode use.

The cyclic variations of beam efficiency which occur during the first few hours of cathode age are illustrated in Figure 23 by the curves of beam-current as a function of cathode age, with total discharge-current maintained constant at 3.0 milliamperes. Curve A gives the beam-current from a cathode which was aged without using the fore-concentration field at any time. Data for curve B were obtained by using the fore-concentration field current which gave maximum beam increase at all times except while data for curve C were being obtained. The needle valve leak was re-adjusted each time a change was made from curve B to curve C so that discharge-current was constant at all times. No wide variations of needle valve setting were made while obtaining the data for curve A. Earlier tests indicated that there might be a systematic increase of total discharge-current when the beam-current was increasing, and a less definite decrease of total discharge-current when the curve had a negative slope. This was corrected by adjusting the needle valve leak slightly to maintain a constant total discharge-current. Attempts to check such a variation of the total discharge-current were unsuccessful because the needle valve assembly developed an erratic leak which masked the smaller variations of total discharge-current.

Allowing the cathode to age without correcting the changing discharge-current does not eliminate the cyclic efficiency variations. If the cathode is moved, even slightly, after the beam efficiency has become steady, the beam-current will decrease greatly, then recover as a

new crater is formed by eroding a side of the old crater. No evidence of more than a single fluctuation was observed, although it is possible that several might occur.

A crater does not form immediately when a new cathode is installed, but forms after a delay of approximately 5 minutes. This time corresponds to the first sharp maximum in the beam-current curve. Two independent experiments confirm this observation. The surface of the cathode can be observed, using the oscillograph as an electron microscope, and no indication of a crater exists during the first few minutes of use. Or, the cathode may be removed after a few minutes use, and a matte surface has been formed on the cathode by the bombardment of the positive ions, but a crater has not yet been developed.

The beginning of a crater is also dependent on the condition of the cathode surface when a discharge is first started. One cathode gave a beam current of 38 microamperes at an age of 1 minute, a maximum of 62 microamperes at an age of 5 minutes, 34 microamperes at an age of 10 minutes, and 8 microamperes at an age of 16 minutes. Another cathode, which was accidentally subjected to a high-pressure glow discharge when first installed, gave a beam-current of 8 microamperes at an age of 2 minutes, reached a maximum of 30 microamperes at an age of 13 minutes, and the beam-current had decreased to 24 microamperes at an age of 18 minutes. Both cathodes were aged with a total discharge-current of 3.0 milliamperes. Both cathodes gave a steady beam-current of 25 microamperes after they had been operated continuously for 6 hours. These data refer to the beam-current without any fore-concentration field, although a fore-concentration field was used at other times during the tests.

The weight of material lost by the cathode as a crater is formed is proportional to the time the cathode has been used, and within the

possible accuracy of measurement, seems to be the same for a cathode aged without fore-concentration, and a cathode aged with a fore-concentration field applied continuously. Average weight of the cathodes used was 170 milligrams and the weight loss was about 1.5 milligrams during 10 hours of operation. The sputtered material is deposited on the cooled walls of the discharge chamber, probably in the form of aluminum oxide.

WRITING SPEED

Three factors may limit the useful writing speed of a cathode-ray oscillograph. The electron energy may be too low to permit satisfactory observation or photography with the beam. The transit time of the electrons past the deflection system may become long relative to the period of the voltage variation being measured and introduce amplitude distortion. If a sinusoidal voltage variation of a period equal to the transit time is applied to the deflection plates, this distortion will produce zero deflection. The third factor is the natural frequency of the deflection system itself. Any instrument is limited as a measuring device if the period of the measured variation corresponds to the natural period of the instrument.

These three factors become important almost simultaneously in the oscillograph under consideration. The electron energy available permits a writing speed of 2×10^9 cm. per second. This writing speed is obtained if the recorded amplitude of oscillations at the natural frequency of the deflection plates and leads just fills the field of the camera. The transit time of the electrons, neglecting relativistic corrections which are not great for a beam with an energy of 10000 electron volts, can be obtained from:

$$\tfrac{1}{2}mv^2 = eV$$

$$v = \sqrt{\frac{2e}{m}V} = 6 \times 10^9 \text{ cm/sec.}$$

$$t = \frac{s}{v} = \frac{6}{6 \times 10^9} = 1 \times 10^{-9} \text{ sec.}$$

where s is the length of the deflection plates, in this case, 6 cm. The natural frequency of the deflection system is approximately 125 megacycles per second, so the natural period is:

$$T = \frac{1}{f} = \frac{1}{125 \times 10^6} = 8 \times 10^{-9} \text{ seconds}$$

and the transit time of the electrons in the beam is sufficiently small to prevent amplitude distortion for any frequencies which can be measured with the oscillograph.

The maximum writing speed was obtained by connecting both deflection plate terminals to a small capacity with the shortest possible leads. Coupling leads to the blocking gap, isolated by coupling condensers, were connected directly to the deflection plate terminals to obtain Figure 24, and were coupled to the deflection plate terminals by small capacities made by twisting two insulated wires together when Figure 25 was photographed. Discharge-current for these photographs was 3.0 milliamperes, and the current in the beam, with fore-concentration, was 88 microamperes. A sweep circuit ten times faster than the fastest sweep normally available with the oscillograph was constructed for these tests.

Writing speed is defined as the ratio of the length of the trace to the corresponding value of the elapsed time. For a sinusoidal wave form, the maximum writing speed may be computed from:

$$\frac{dx}{dt} = \frac{d}{dt} A \sin 2\pi ft = 2\pi fA \cos 2\pi ft$$

where A is the amplitude of the deflection. The above equation gives the correct maximum writing speed only if the trace is nearly perpendicular to

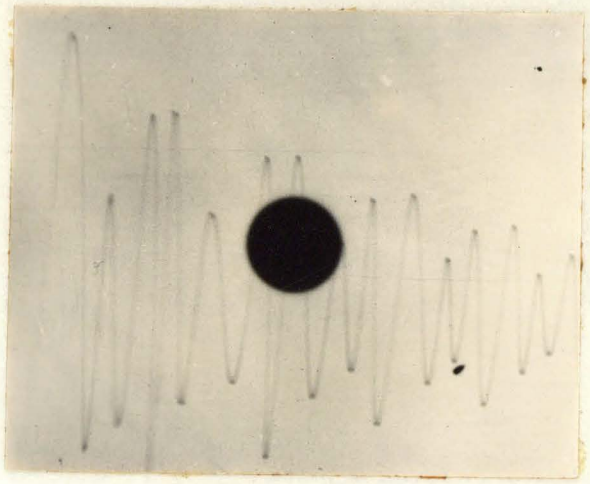

Figure 24
125 megacycles
Natural frequency of deflection plates

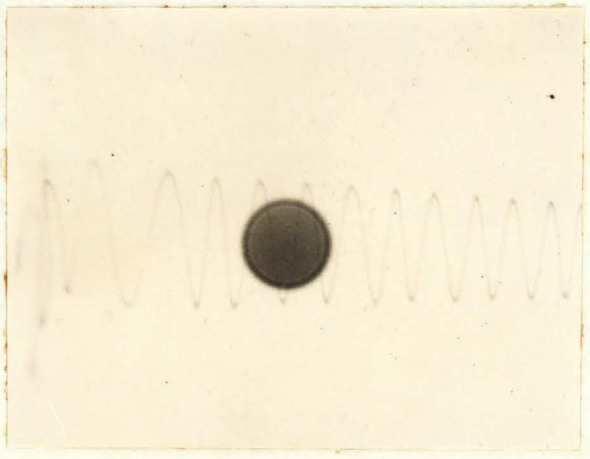

Figure 25
125 megacycles
Natural frequency of deflection plates

the direction of sweep. Substitution of 125 megacycles per second for the frequency gives a maximum writing speed somewhat greater than 2×10^9 cm/sec. for Figure 24, and 8×10^8 cm/sec. for Figure 25. These values are greater than those quoted by R. H. Griest[1]. The improvement is due primarily to the reduction of beam distortion.

RECOMMENDATIONS

One conclusion is obvious - a better vacuum system is necessary. The present mercury vapor pumps might be improved by cleaning, and would be improved if jets of newer design were installed. But the advantages of modern oil diffusion pumps make the replacement of the present pumps desirable. One precaution is necessary. Oil diffusion pumps are damaged and may even become inoperative if a large amount of water vapor comes in contact with the heated oil. Certain oil diffusion pumps are self-fractionating and might be used to remove the moisture from the films if the oil were replaced frequently. Using the present vacuum pumps to remove the water vapor from the films before they are placed in the oscillograph, and installation of a new, larger fore-pump and adequate oil diffusion pumps would be preferable. A liquid air vapor trap at the air inlet to the needle valve leak would also be desirable, as the humidity of the atmosphere becomes quite high occasionally.

The cathode assembly could be improved by substituting a glass to kovar seal for the present mica-picein seal. This change might be accomplished without any revision of the metal parts of the present assembly. Elimination of one source of vacuum trouble and more exact and permanent centering of the cathode would be the result. Substitution of rubber gaskets for other wax joints should be considered.

Additional data on the behavior of the discharge as a cathode is aged are desirable. The aluminum deposit on the walls of the discharge tube has been removed since the data for Figure 23 were obtained. Similar tests of beam-current as a function of cathode age should be repeated in order to determine the effect of the changed dimensions of the discharge chamber on the anomalous behavior of the beam-current. If the phenomenon

persists, a series of cathodes might be removed at different ages and examined microscopically to determine whether the shape of the cathode crater varies cyclicly with the variations of beam efficiency. Information regarding the behavior of a cold cathode discharge might be obtained from continued investigation of this anomaly.

BIBLIOGRAPHY

1. R. H. Griest: A Low Voltage High-Speed Cathode-Ray Oscillograph. Thesis for Ph.D. degree, California Institute of Technology, 1937.

2. P. F. Hawley: Design and Operation of a Cathode-Ray Oscillograph for External Photography. Thesis for Ph.D. degree, California Institute of Technology, 1936.

3. J. G. Pleasants: Observations on the Theory and Characteristics of Electrical Figures on Plates in Air. Thesis for Ph.D. degree, California Institute of Technology, 1933.

4. W. G. Dow: Fundamentals of Engineering Electronics. John Wiley and Sons, Inc., New York, 1937.

5. W. R. Smythe: Static and Dynamic Electricity. McGraw-Hill Book Company, Inc., New York, 1939.

6. L. B. Loeb: Fundamental Processes of Electrical Discharges in Gases. John Wiley and Sons, Inc., New York, 1939.

7. L. M. Myers: Electron Optics - Theoretical and Practical. Chapman and Hall, Ltd., London, 1939.

8. I. G. Maloff and D. W. Epstein: Electron Optics in Television. McGraw-Hill Book Company, Inc., New York, 1938.

9. A. B. Wood: Cathode-Ray Oscillograph. I. E. E. Journal, Vol. 63, p. 1046, November 1935.

10. J. B. Johnson: The Cathode-Ray Oscillograph. Journal of the Franklin Institute, Vol. 212, p.p. 687-717, December 1931.

11. M. von Ardenne: Untersuchen an Braunschen Röhren mit Gasfüllung. Hochfrequenztechnik und Elektroakustic, Vol. 39, pp. 18-24, 1932.

12. H. Busch: Über die Wirkungsweise der Konzentrierungsspule bei der Braunschen Röhre. Archiv für Elektrotechnik, Vol. 18, p. 583, 1927.

13. V. K. Zworykin: On Electron Optics. Journal of the Franklin Institute, Vol. 215, p. 535, May 1933.

14. E. Ruska: Bau und Leistung des magnetischen Elektronenmikroskops. Zeitschrift fur Physik, Vol. 87, pp. 580-602, 1934.

APPENDIX A

"Ionization Times of Thyratrons"

By

Arthur E. Harrison

AIEE
Technical Paper
39-116

April 1939

IONIZATION TIME OF THYRATRONS

A. E. Harrison
Enrolled Student
California Institute of Technology,
Pasadena

A paper recommended by the AIEE subcommittee on electronics and scheduled for presentation at the AIEE combined summer and Pacific Coast convention, San Francisco, Calif., June 26-30, 1939. Manuscript submitted February 16, 1939; made available for preprinting April 25, 1939.

IONIZATION TIME OF THYRATRONS

By
A. E. Harrison

SUMMARY

enteen thyratron and grid glow tubes, representing 12 different types, have been and their ionization times have been measured with a cold cathode type oscillograph. nization times vary over a wide range, from a fraction of a microsecond to several microseconds. Ionization time has been found empirically to be inversely propor- o grid overvoltage. Grid overvoltage is defined as the difference between the l applied to the grid and the critical potential necessary to prevent firing. Argon, d mercury vapor tubes were included in the test. Mercury temperature was found to appreciable effect on the ionization time with low grid overvoltages. All mercury bes have similar ionization time characteristics. In fact, tubes of the same type facture sometimes differed from each other more than one tube differed from another different construction and manufacture.

---

d controlled vapor filled rectifiers, or thyratrons, have not been considered in the use in blocking and sweep circuits for cold cathode type oscillographs because of herent ionization time. A search of the literature on the subject, and reference to urers' data sheets furnished little useful information on this ionization time. A program to determine the minimum ionization times of various tubes was thus started and first results showed that minimum ionization times of 0.3 microseconds were le with mercury vapor thyratrons if the grid was driven sufficiently positive. These suggested that these tubes might be successfully used in blocking circuits for high cillographs, and work on this phase of the problem is being continued. The apparatus for measuring ionization times made possible an extended study of the relation be- nization time and grid overvoltage as a function of anode voltage and vapor temperature, cury tubes) and it is the results of this extension of the original problem which discussed.

EXPERIMENTAL PROCEDURE

ization time of a thyratron, or the delay between the time of application of a square ulse to the grid and the time the tube voltage reaches its normal conducting value, y measured with a high speed cathode ray oscillograph arranged to record the voltage he tube, provided that the time of application of the grid impulse is also shown. cessary to synchronize the unblocking of the high speed oscillograph with the trip- ulse applied to the tube under test. (Tube B in Figure 1.) This is accomplished se of a trip tube (Tube A) which is fired by a surge from the oscillograph blocking delayed a fraction of a microsecond by R_5C_G. An impulse of magnitude determined atio of $R_3/(R_3+R_4)$ is applied to the grid of the tube under test when tube A fires. ulse voltages from 3 to 63 volts are selected with a tap switch connected to differ- es of R_3, allowing the grid overvoltage, or difference between the potential ap- the grid and the critical potential necessary to prevent firing, to be varied over ange. The time of application of grid impulse is recorded on the oscillogram through ling capacity C_4. C_4 and C_5 are small coupling capacities formed by 1 inch of twisted insulated wires.

ues of grid impulse voltage were calculated from the ratios of $R_3/(R_3+R_4)$ for the taps and were checked with the cathode ray oscillograph. The apparatus was mounted the oscillograph as possible (See Figure 2) in order to reduce the length of leads. th the oscillograph verified that the time constant of R_4 and the grid to cathode of tube B had no appreciable effect on the measurement of the ionization time.

First tests were made with the tube under test in a circuit similar to that of tube A without R_5 , and ionization times were measured from the beginning of the oscillogram. Two factors made such a simple circuit unsatisfactory; there was no control of grid overvoltage independent of initial grid bias, and tests with an 885 indicated that the delay in the blocking circuit of the oscillograph was greater than the minimum ionization time of this tube. Both drawbacks were eliminated by the addition of a trip tube to the circuit. An 885 tube was finally chosen as a trip tube because its breakdown time was quite short and gave the best approach to a true square wave impulse. R_5 was therefore added to delay the trip until the oscillograph sweep had started.

Direct coupling and capacitive coupling to the grid of tube B were tried and capacitive coupling was finally adopted because it allowed control of initial grid bias with a potentiometer and frequent check of the critical bias was possible. Originally, carbon resistors were used for R_3 and R_4 ; but this type of resistance has an odd behavior under transient conditions and the grid impulse voltage could not be calculated from the d.c. resistance of the carbon units. Metallized resistor units for R_3 and ten metallized resistor units approximately 400 ohms each in series for R_4 overcame this difficulty, giving a voltage divider with approximately the same characteristics for d.c. and transient conditions.

Condensed mercury temperatures were measured with a mercury thermometer wrapped with tinfoil and tied against the base of the bulb. This method did not give accurate measurement of the temperature, and did not allow tests at subnormal vapor temperatures, but the results do indicate qualitatively the effects of changes in mercury temperature.

Test data were obtained photographically for the 12 types of tubes listed in Table I after the tubes had reached an equilibrium temperature. Three or more oscillograms were taken for each value of grid overvoltage and a fixed anode voltage. The sensitivity of the oscillograph was such that anode voltages greater than 1000 volts could not be recorded easily. The time base was calibrated with a radio frequency oscillator which was checked against broadcast stations. Figures 3 and 4 are representative oscillograms of anode to cathode potential. Ionization time is measured from the time of application of grid impulse, recorded as a slight rise in voltage at the beginning of the oscillogram, to the time at which the tube voltage has dropped to its conducting value. The ionization time for the strobotron was an exception, since a strobotron is used without a load resistance to discharge a condenser, and its ionization time was measured to the beginning of breakdown.

EXPERIMENTAL RESULTS

Ionization time as a function of grid overvoltage has been plotted in Figure 5 for six of the tubes listed in Table I. Inspection of the curves of Figure 5 suggests a resemblance to a family of rectangular hyperbolas. Figure 6 was prepared to check this suggestion and shows the reciprocal of ionization time plotted as a function of grid overvoltage. The resulting curves are nearly linear, indicating that the hyperbolic form of the curves in Figure 5 is not an illusion. The greatest deviation from linearity is shown by the FG-81; but this is not surprising since the maximum grid overvoltage is high compared with the anode voltage. All of the argon filled tubes reached a low value of ionization time with a grid overvoltage of 20 or 30 volts, and further increase of grid impulse voltage failed to reduce the ionization time appreciably. V. C. Rideout, graduate student at the California Institute who is continuing this study, has varied grid bias, grid impulse voltage, and anode voltage proportionately in an attempt to maintain proportional gradient values for each test. His conclusions are not yet definite, but there is reason to believe that this technique gives reciprocal curves which are more nearly linear.

Published data regarding the ionization times of thyratrons are meager. Hans Klemperer[1] in 1932 suggested a theory based on the mobility of the positive ions, and his calculated ionization times agreed in magnitude with his observations. Unfortunately the magnitude of the positive impulse applied to the grid by his method was not given, although it apparently was large. Klemperer's theory predicts that the time from the application of grid overvoltage until the start of voltage decrease across the tube, (T_1 in Figure 4) and the time for the anode voltage to reach its final conducting value after decrease across the

tube has begun, T_2 , should be approximately equal. This relation is true for large grid overvoltages, but it is definitely not true for low grid overvoltages. The ionization time may depend on the initial number of electrons available to cause ionization, the so-called dark electron current.[4],[6] Some vapor tubes have much larger dark electron currents just before breakdown than others. Figure 4 indicates the existence of a relatively large electron current by a gradual drop in anode voltage before final breakdown. No change in the ionization time of a KY-21 was observed when R_2 was changed from 20,000 ohms to 2,000 ohms if the grid overvoltage was greater than 5 volts. There is a substantial reduction in the ionization time for grid overvoltages of 2 or 3 volts, however, when the load resistance is reduced. As yet, a theory to predict or explain the observed relation between ionization time and grid overvoltage has not been suggested.

Observations regarding individual tubes may be interesting. The electrode construction of an 885 differs radically from that of the other tubes and this thyratron has a very short ionization time, practically independent of anode voltage. In comparison with an 885, a 2A4G has much longer ionization times at low grid overvoltages, but the ionization times are almost identical at the higher grid overvoltages. Compare Figure 7 and curve A in Figure 5. An FG-81, however, has a ionization time curve more nearly like that of the mercury vapor tubes, although it is argon filled. Ionization times for neon filled tubes were in all cases longer than the ionization times of argon or mercury vapor tubes. Two KU-610 tubes were tested and gave slightly different results with 750 volts applied to the anode. These tubes would not operate consistently at anode voltages less than 500. These were old tubes, however, and this behavior may not be caused by the use of neon gas. Direct comparison of tubes filled with noble gases could not be made because the ionization times are affected by gas densities in the tubes and these were not known.

All tubes except the 885 show a variation of ionization time characteristic with different anode voltages. In all cases where anode voltage affected the ionization time curve, an increase of anode voltage caused the knee of the curve to be more pronounced. Figures 7, 8, and 9 illustrate this effect for three types of tubes. The longer ionization time for large grid overvoltages with 100 volts on the anode is due primarily to an increase in the breakdown time (T_2 in Figure 4), as the time lag T_1 is practically the same for all anode voltages when grid overvoltage is large. Note that there is little difference between the curves for an FG-57 and a KY-21 in Figures 8 and 9. A second FG-57 showed ionization times consistently longer than those for the KY-21. It is common for mercury vapor tubes of the same type and manufacture to differ from each other in characteristics, more than one differs from another tube of different construction and manufacture.

No change in the ionization time of several mercury vapor tubes was found when the tube was biased to a large negative value (-50 volts bias for a tube with a critical bias of -5 volts) and the positive grid impulse increased so that the grid overvoltage was the same as before. Other circuits may give ionization times much longer than the values given here if they use high grid limiting resistors which introduce an additional RC lag.

An unusual phenomenon was observed while testing an 866 which had a special shield electrode placed around the cathode. The critical bias necessary with 400 volts on the anode changed within a few hours use from -4 volts to -60 volts. Loss of grid control continued as long as the filament was heated, although the anode voltage was zero and the grid bias -60 volts. A. W. Hull[2] mentioned this effect in 1929. The tube mentioned above was new, but the construction may be incorrect for use as a thyratron.

In some tubes, particularly the FG-17, a variation of ionization time for a given low grid overvoltage and low anode voltage was observed. The special 866 and the KY-21 also showed this effect, but the spread of ionization times was not as wide. An anode voltage of 300 reduced the variation, and 1000 volts on the anode practically eliminated the effect. All of these tubes have filament type cathodes and the effect is probably related to changes in effective cathode potential for different parts of the cycle. A difference in emissivity for different parts of the filament would exaggerate the effect, although the center of the filament supply might be at ground potential. The FG-17 tubes were several years old and probably not in the best condition, which may account for their pronounced variation of ionization time for a given low grid overvoltage.

Variation of the ionization time characteristic of an FG-57 operated with an anode voltage of 300 is shown for three different mercury temperatures in Figure 10. Mercury temperature has considerable effect at the higher grid overvoltages, but the curves coincide for low grid overvoltages. The temperatures indicated are not necessarily accurate, as they were measured by a questionable method. In fact, a series of tests with different temperatures and a fixed value of grid overvoltage gave erratic results. But each of the three curves in Figure 10 represents a consistent set of data for some temperature, and the trend is certainly definite. Changes in temperature produce a similar effect on the ionization time curves of all the mercury vapor tubes.

Two cold cathode tubes were tested. The OA4G is argon filled and its maximum ionization time is very long. The strobotron is a neon filled, cold cathode tube, and cannot be compared directly with the other hot cathode types. It is interesting to note, however, that the curve for the strobotron resembles the curve for the KU-610, a hot cathode neon filled tube, if the curves are displaced vertically until the minimum ionization times are equal. (Figure 5). Perhaps this is an indication that there is a fixed time lag necessary for initiation of emission, although the data are not sufficiently complete to prove this theory. Two values of capacitance were used across the anode and cathode of the strobotron and the load resistor (R_2 in Figure 1) was zero. Two microseconds were required to discharge a 1 microfarad condenser, and eight microseconds were required to discharge a 10 microfarad condenser. These values are the time required for the condenser to discharge. Discharge occurs after a delay, depending on grid overvoltage, as given in curve F, Figure 5.

The results of these investigations show that the ionization time of mercury vapor thyratrons may be as short as 0.3 microseconds if a positive impulse of sufficient magnitude is applied to the grid. Certain argon filled types have even shorter ionization times. Characteristics of tubes of the same type may vary more than characteristics of tubes of slightly different construction. All tubes show the same general relation between ionization time and grid overvoltage. For most tubes the ionization time is inversely proportional to the grid overvoltage. There has been no theory suggested to explain this observed relation. However, these empirical data can be the basis for practical application and further investigation.

BIBLIOGRAPHY

1. ÜBER DEN ZEITLICHEN VERLAUF DER ZÜNDUNG VON IONENROHREN, Hans Klemperer, Archiv für Electrotechnik, volume 27, 1933, pp. 322-328.

2. THYRATRONS, HOT CATHODE, A. W. Hull, General Electric Review, volume 32, April 1929, pp. 213-223.

3. IONIZATION TIME OF THYRATRONS, L. B. Snoddy, Physics, volume 4, October 1933, pp. 366-371.

4. PRE-STRIKING CURRENTS IN A THYRATRON, E. T. Wheatcroft, R. B. Smith, J. Metcalfe, Philosophical Magazine, volume 25, April 1938, pp. 649-663; also E. T. Wheatcroft and T. G. Hammerton, Philosophical Magazine, volume 26, November 1938, pp. 684-694.

5. ELECTRONICS AND ELECTRON TUBES, a book, E. D. McArthur, John Wiley and Sons, Inc., 1936.

6. FUNDAMENTALS OF ENGINEERING ELECTRONICS, a book, William G. Dow, John Wiley and Sons, Inc., 1937. Includes a good bibliography.

7. ADDITIONAL BIBLIOGRAPHY ON VAPOR TUBES, General Electric Review, volume 41, October 1938, page 456.

TABLE I

RANGE OF IONIZATION TIMES - MICROSECONDS

Number of Tubes Tested	Tube	Manufacturer	Gas	Anode Voltage	Shortest Measured Ionization Time	Approximate Maximum Ionization Time
		HOT CATHODE TYPES				
2	FG-17	General Electric	Mercury	1000	0.50	50
2	FG-57	General Electric	Mercury	1000	0.40	50
1	FG-67	General Electric	Mercury	1000	0.60	150
1	WE 287-A	Western Electric	Mercury	1000	0.65	50
1	KY-21	Eitel-McCullough	Mercury	1000	0.45	20
1	866 Special	*	Mercury	1000	0.35	20
3	885	RCA	Argon	300	0.08	1
1	2A4G	Raytheon	Argon	300	0.10	10
1	FG-81	General Electric	Argon	180	0.25	50
2	KU-610	Westinghouse	Neon	750	1.80	300
		COLD CATHODE TYPES				
1	0A4G	Raytheon	Argon	300	3.0	300-1000
1	Strobotron	General Radio	Neon	350	12.0	300

* An 866 rectifier with a control electrode added. Manufacturer unknown.

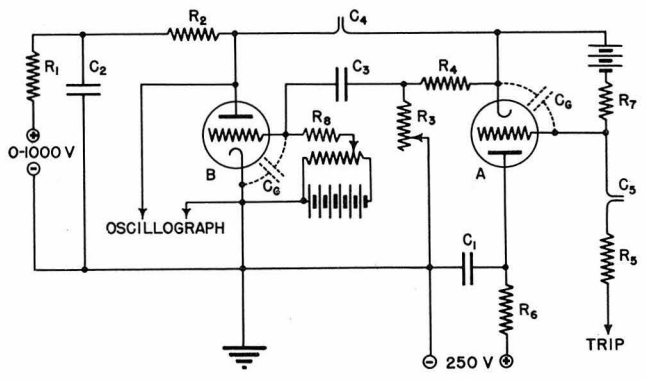

Figure 1. Circuit diagram of thyratron test apparatus

R_1 = 1,000,000 ohms
R_2 = 20,000 ohms
R_3 = 50-1350 ohms
R_4 = 3,700 ohms
R_5 = 100,000 ohms
R_6 = 1,000,000 ohms
R_7 = 1,000,000 ohms
R_8 = 1,000,000 ohms
C_1 = 1 mfd.
C_2 = 1 mfd.
C_3 = 0.001 mfd.
C_4, C_5 } Twisted wire capacities
C_6 = Electrode capacity
Tube A - 885 Thyratron
Tube B - Tube under test

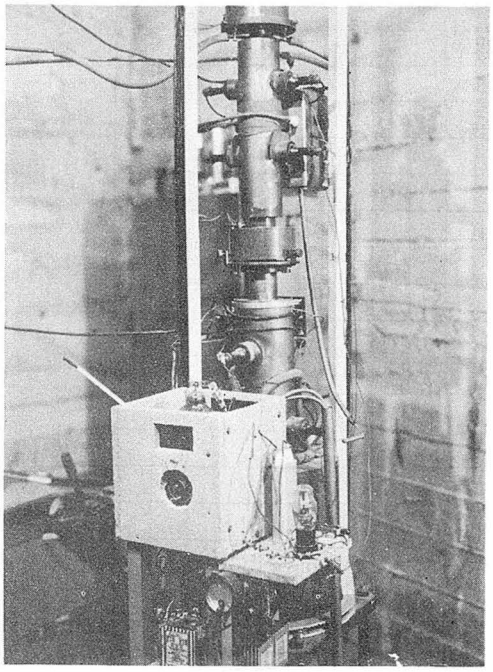

Figure 2. Thyratron test apparatus connected to the high speed oscillograph

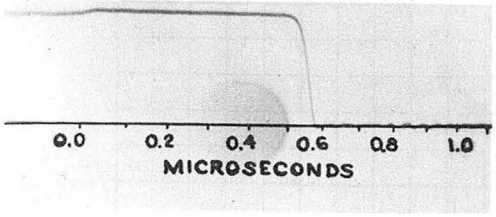

Figure 3. Typical oscillogram for an 885 thyratron

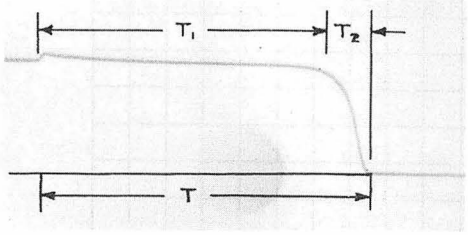

Figure 4. Different phases in breakdown of an FG-57
T_1 = Time lag
T_2 = Breakdown time
T = Ionization time

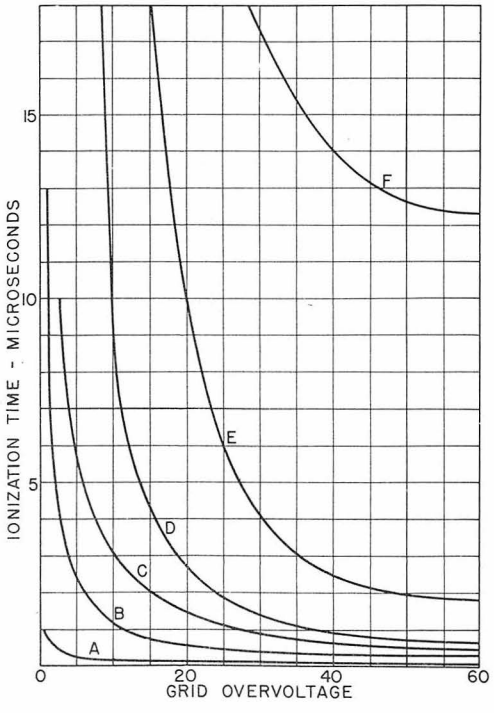

Figure 5. Typical ionization time curves for thyratrons
A - 885 Argon filled thyratron
300 volts on anode
B - FG 81 Argon filled thyratron
180 volts on anode
C - KY 21 Mercury vapor thyratron
1000 volts on anode
D - FG 67 Mercury vapor thyratron
1000 volts on anode
E - KU 610 Neon filled thyratron
750 volts on anode
F - Strobotron - Neon filled, cold cathode
350 volts on anode

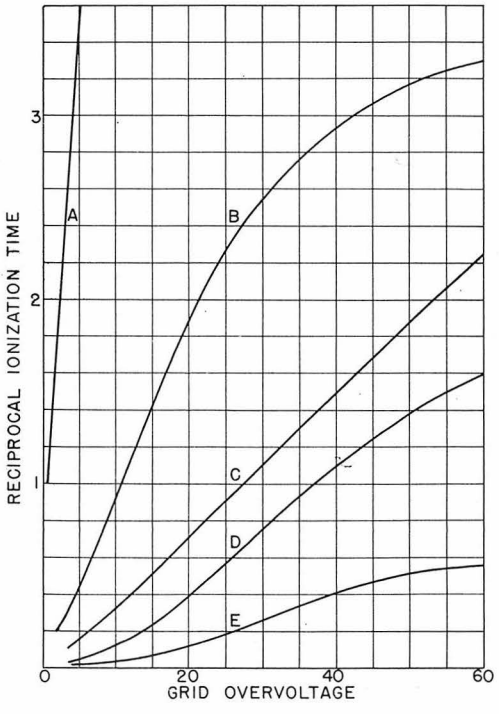

Figure 6. Reciprocal ionization times for Figure 5
A - 885 Argon filled thyratron
300 volts on anode
B - FG 81 Argon filled thyratron
180 volts on anode
C - KY 21 Mercury vapor thyratron
1000 volts on anode
D - FG 67 Mercury vapor thyratron
1000 volts on anode
E - KU 610 Neon filled thyratron
750 volts on anode

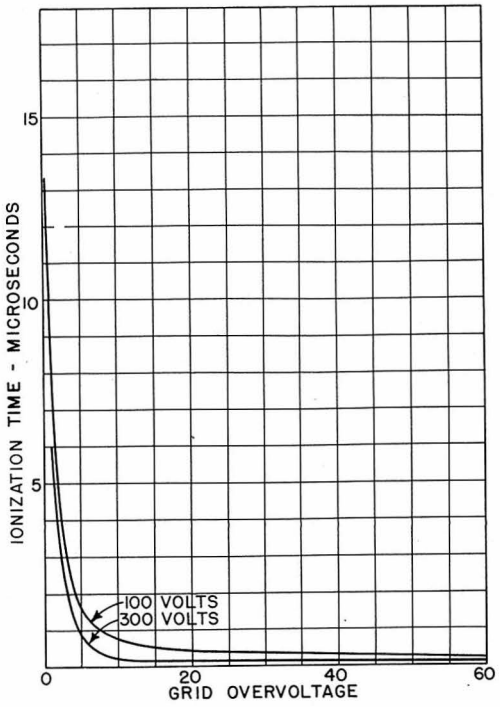

Figure 7. Effect of anode voltage on ionization time of a 2A4 G argon filled thyratron

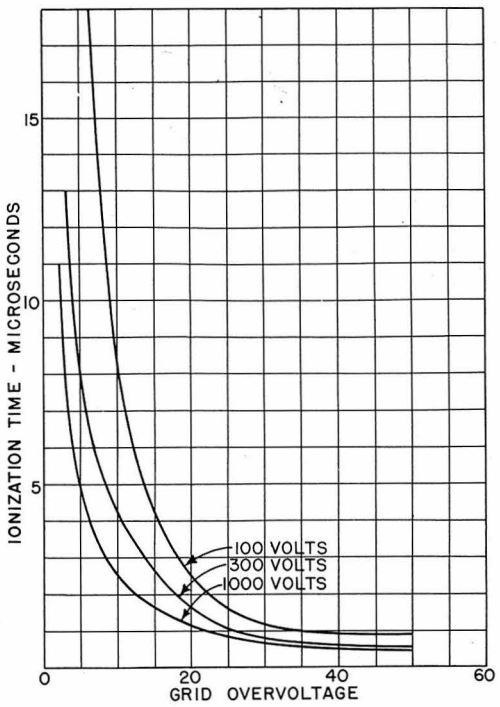

Figure 8. Effect of anode voltage on ionization time of an FG-57 mercury vapor thyratron mercury temperature 70° C

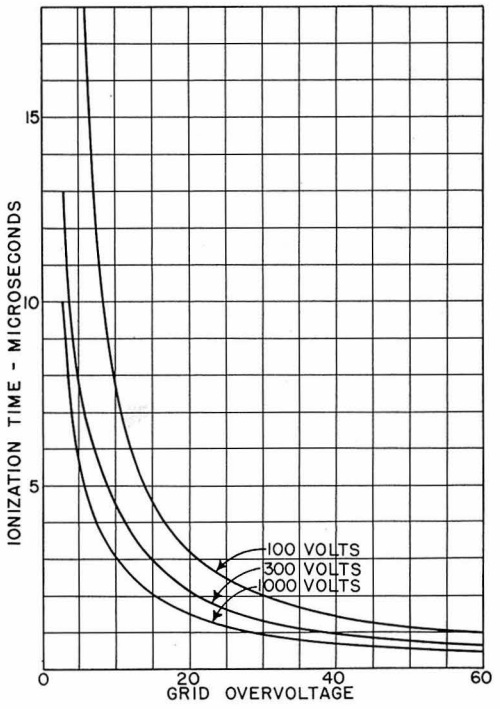

Figure 9. Effect of anode voltage on ionization time of a KY-21 mercury vapor thyratron mercury temperature 67° C

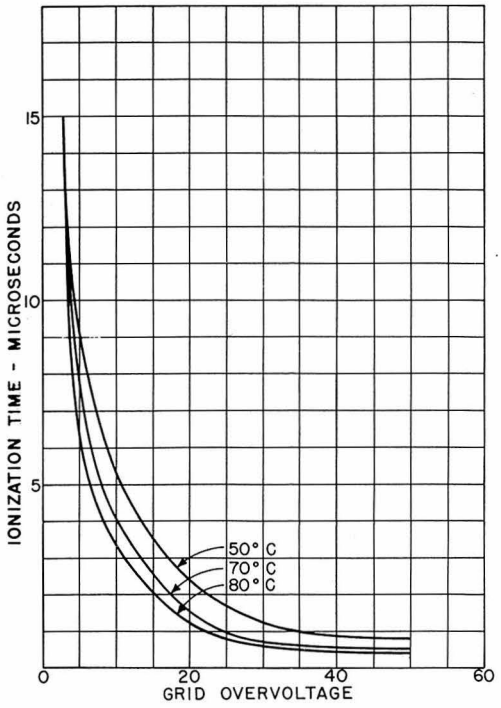

Figure 10. Effect of condensed mercury temperature on ionization time characteristic of an FG-57 with 300 volts on anode

ADDITIONAL DATA ON

"Ionization Times of Thyratrons"

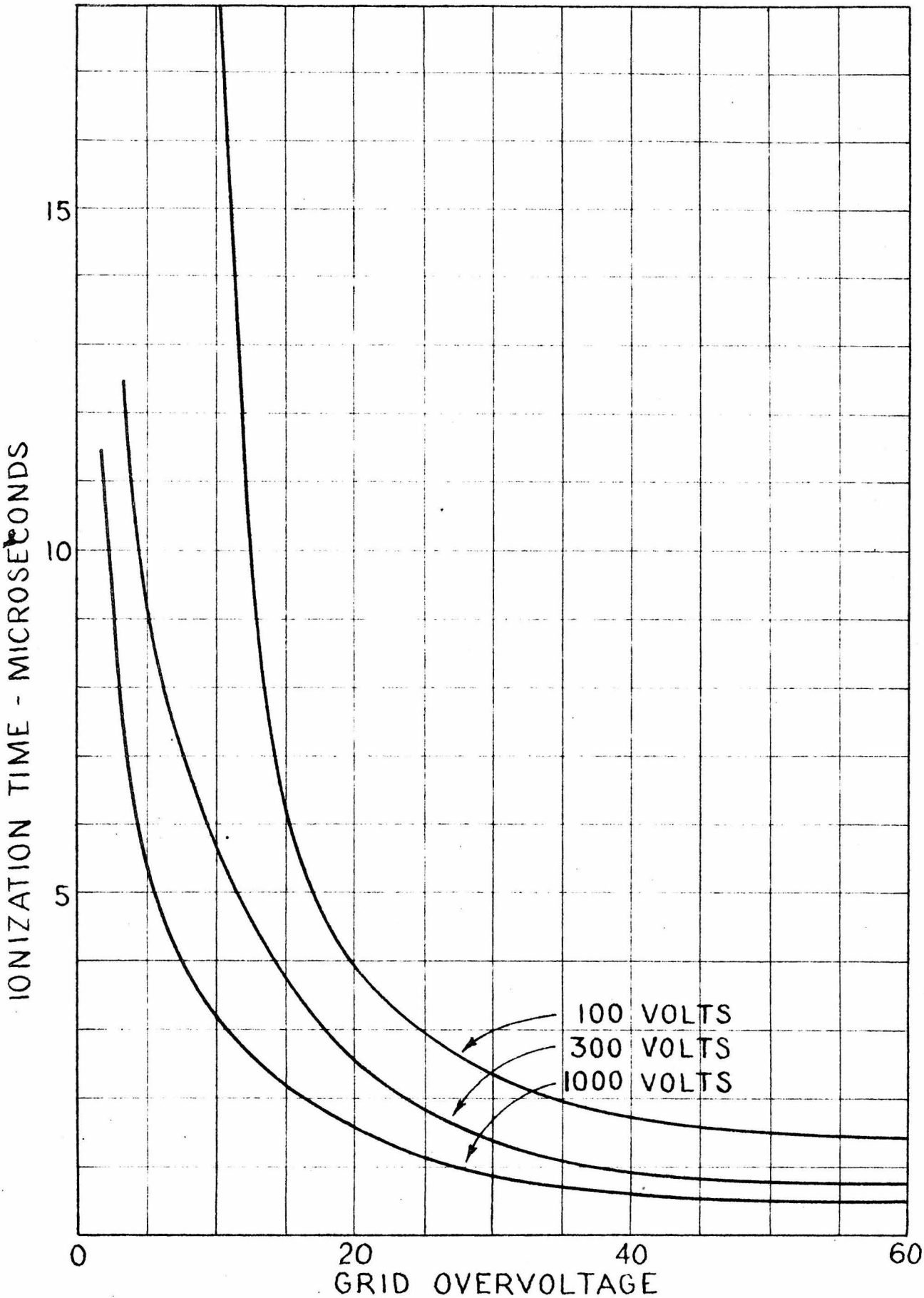

IONIZATION TIMES FG 17 54°C

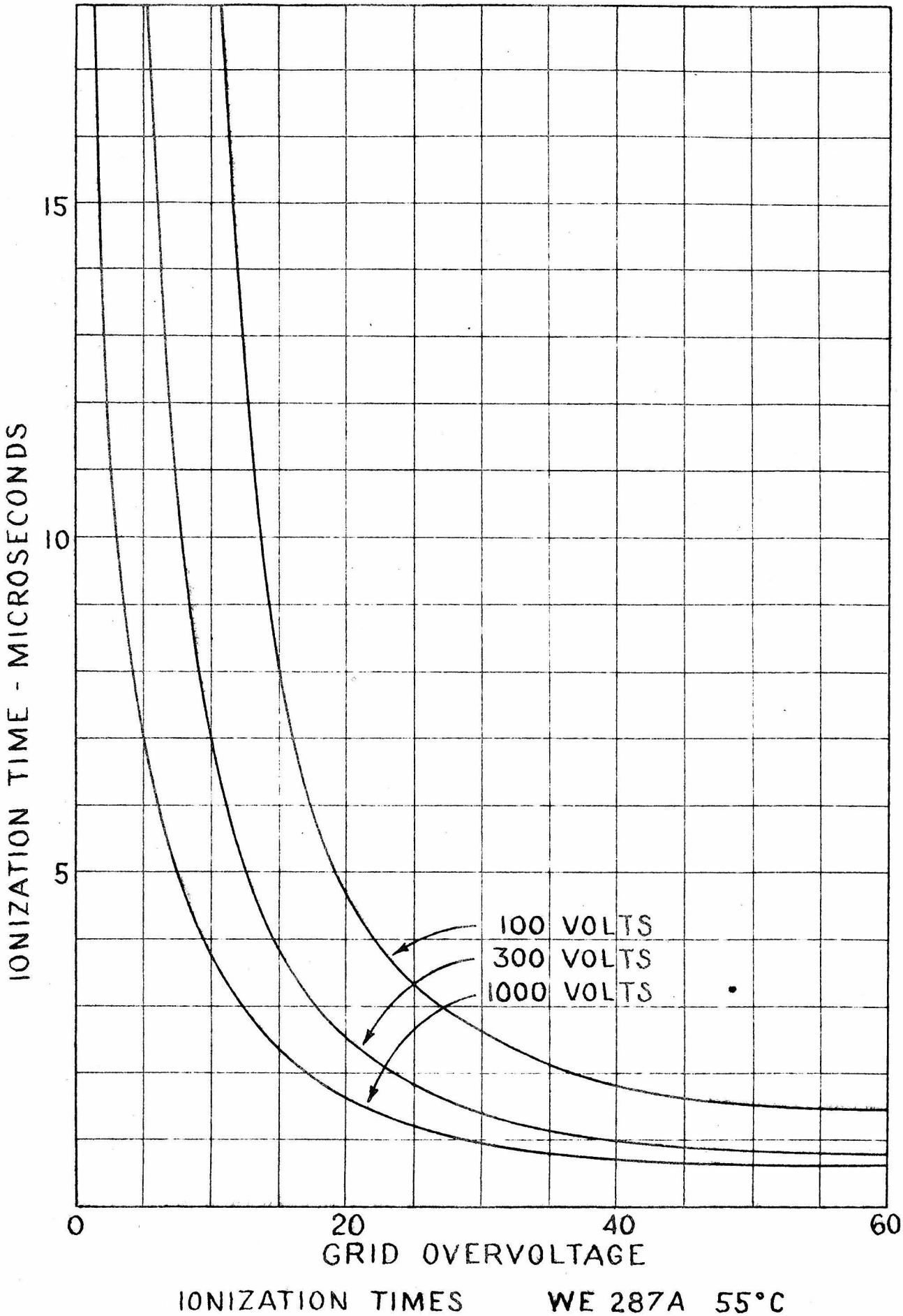

IONIZATION TIMES WE 287A 55°C

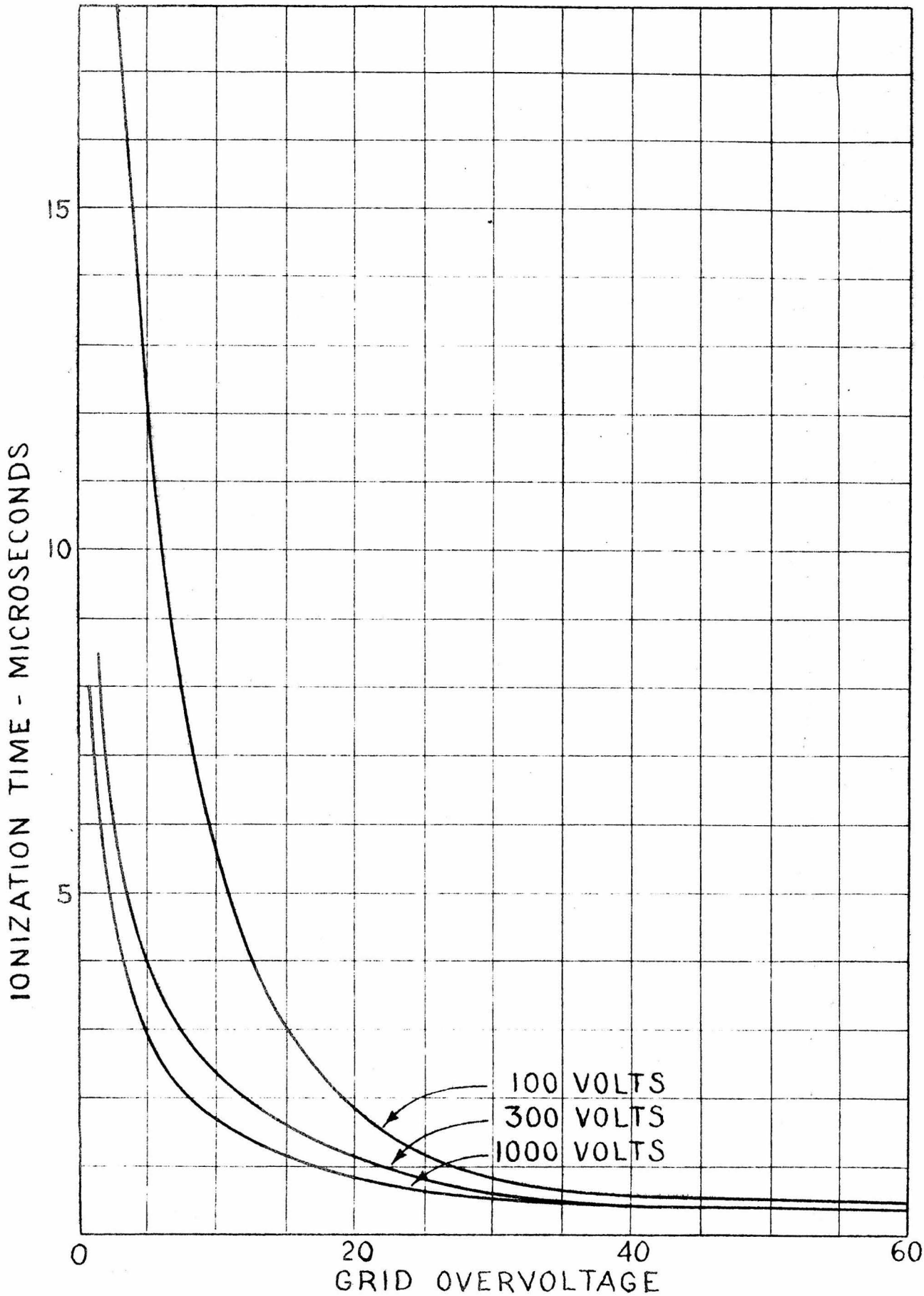

IONIZATION TIMES 866 SPECIAL 65°C

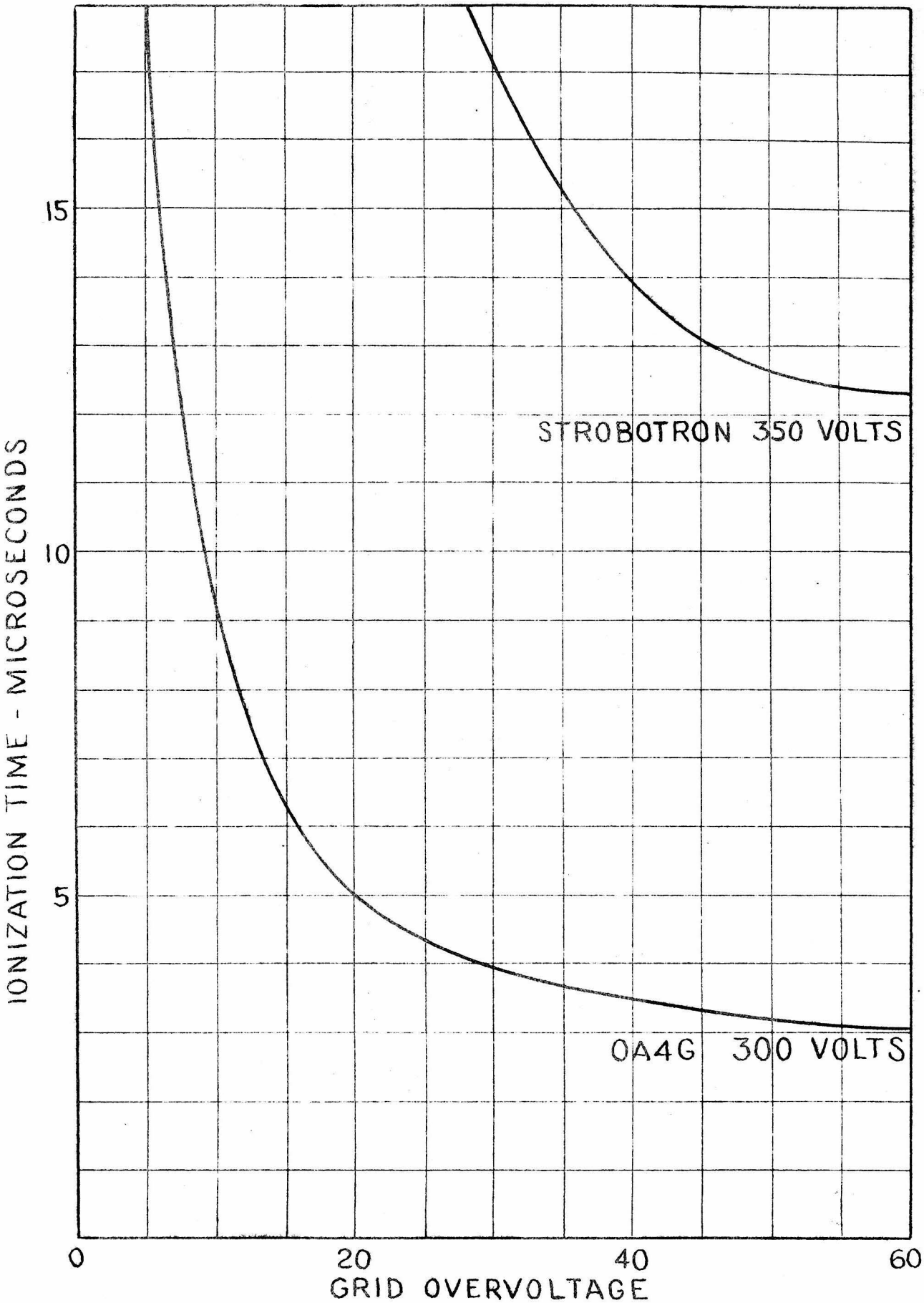

IONIZATION TIMES COLD CATHODE TUBES

APPENDIX B

"Surge Voltage Breakdown Characteristics

for Electrical Gaps in Oil"

By

R. W. Sorensen

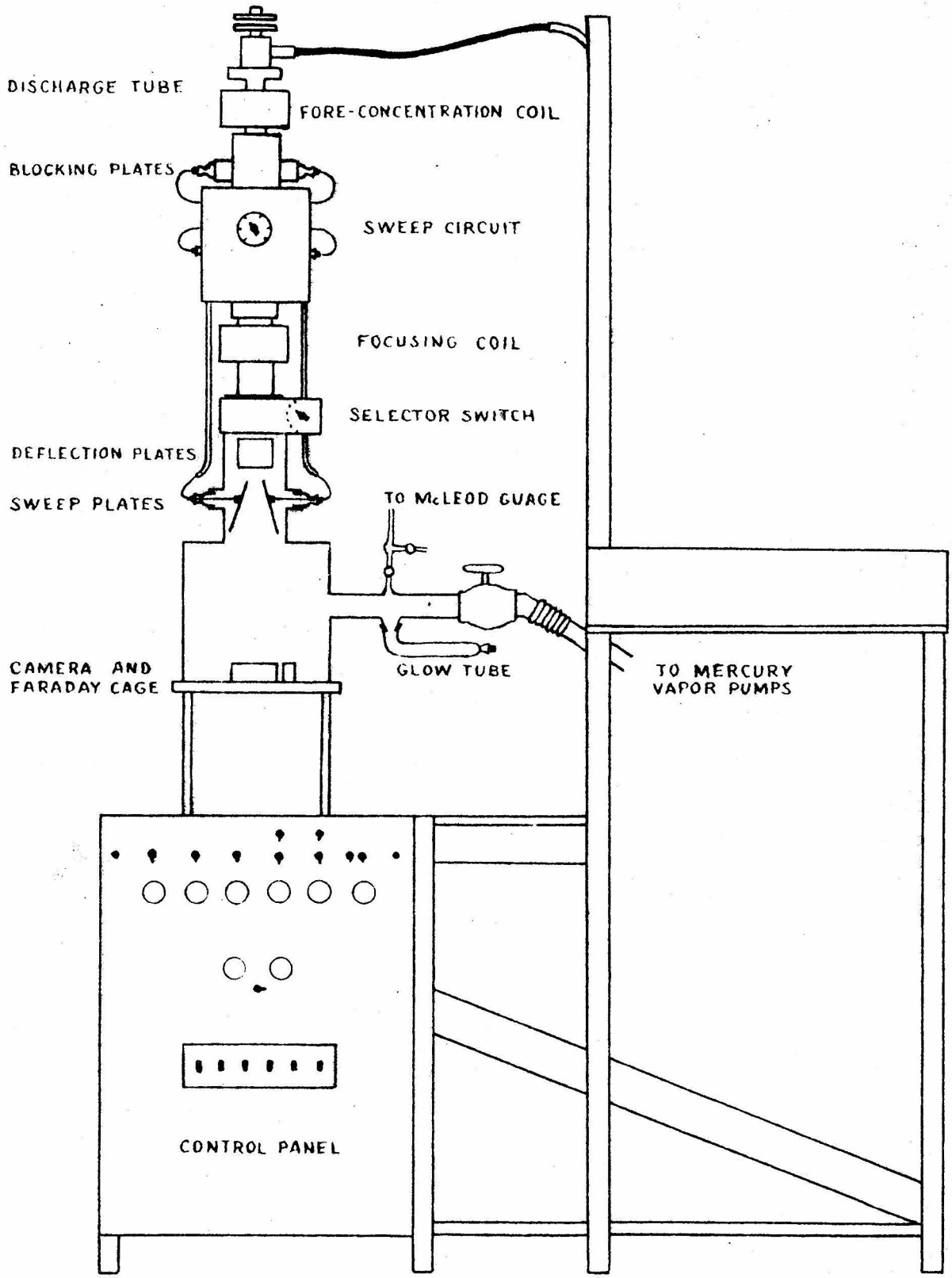

FIGURE 1 OSCILLOGRAPH BENCH

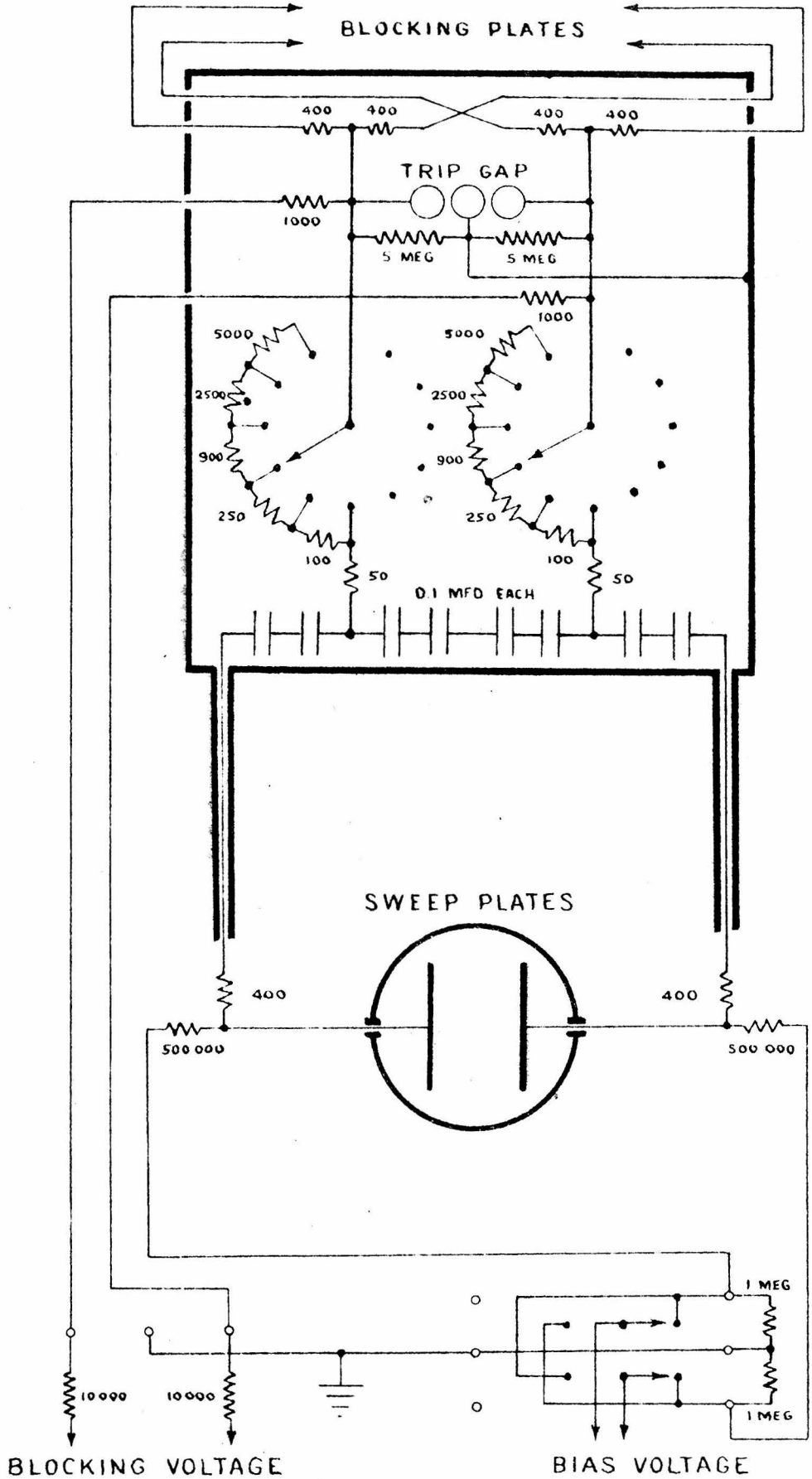

FIGURE 3 SWEEP CIRCUIT

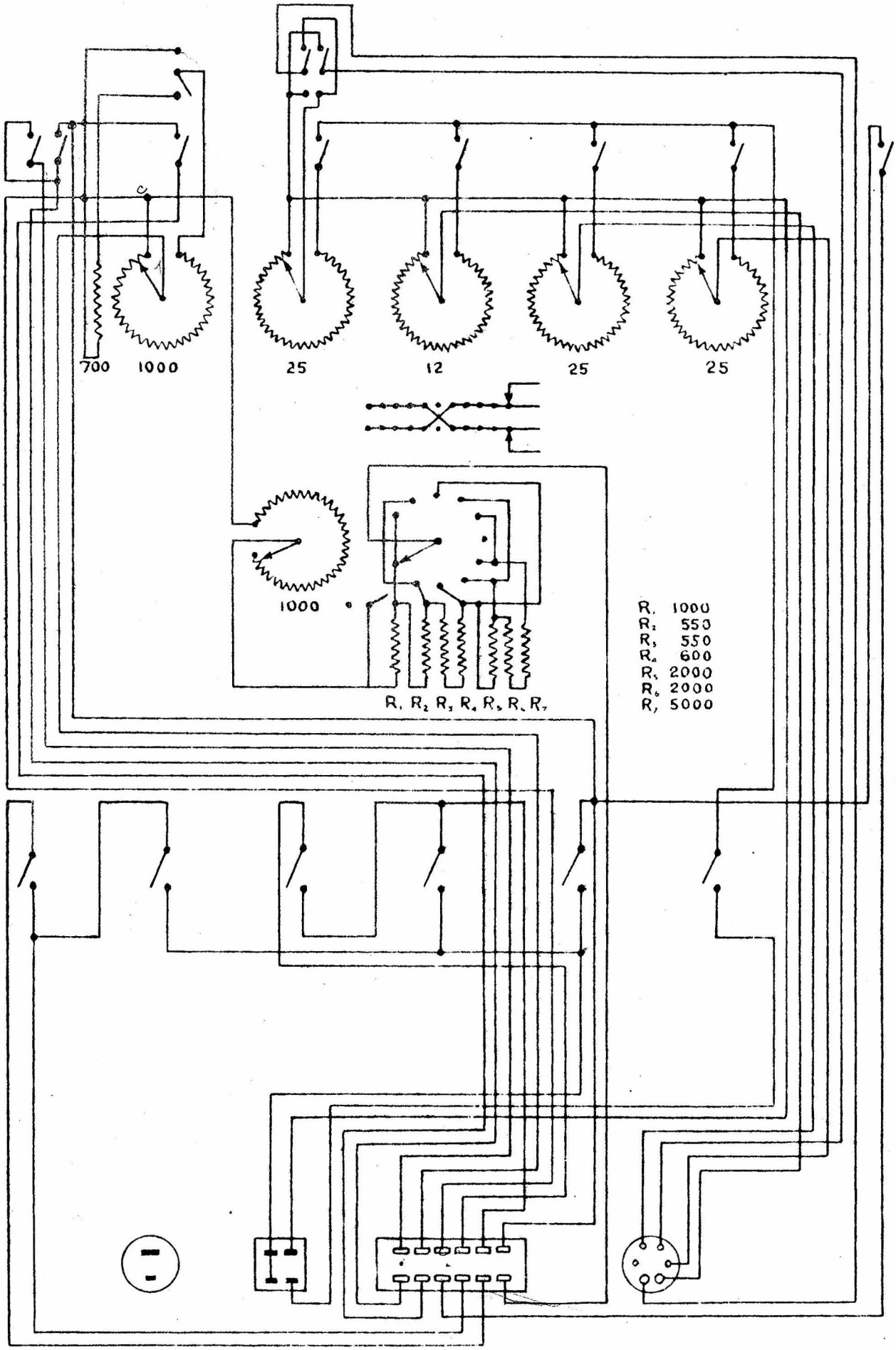

FIGURE 4 CIRCUITS ON CONTROL PANEL